

# Analyzing and Optimizing Denitrification in Agricultural Surface Waters: Spatial and Temporal Analysis of Denitrification Hot Spots

Final Report for  
Minnesota Department of Agriculture  
March 2017

Submitted by:

Jessica Kozarek<sup>1</sup>, Miki Hondzo<sup>1,2</sup>, Michael Sadowsky<sup>3,4</sup>, Abigail Tomasek<sup>1,2</sup>, and  
Nicole Lurndahl<sup>4</sup>

<sup>1</sup>St. Anthony Falls Laboratory, University of Minnesota

<sup>2</sup>Department of Civil, Environmental, and Geo- Engineering, University of Minnesota

<sup>3</sup>BioTechnology Institute, University of Minnesota

<sup>4</sup>Department of Soil, Water and Climate, University of Minnesota



# Contents

Summary.....	ii
Acknowledgements.....	iii
1 Background.....	1
2 Project Goals.....	3
3 Experimental Setup.....	4
3.1 Seven Mile Creek.....	4
3.2 Outdoor StreamLab.....	5
3.3 Flume.....	8
4 Measurement Methods.....	9
4.1 Microbial Measurements.....	12
4.1.1 Gene abundances (DNA).....	12
4.1.2 Microbial community composition.....	15
5 Results.....	16
5.1 Seven Mile Creek.....	16
5.1.1 Environmental parameters and denitrification rates.....	16
5.1.2 Denitrifying gene abundances.....	19
5.1.3 Seasonal DeN and DEA trends.....	20
5.1.4 Coupling between denitrifying gene abundances, denitrification rates, and environmental parameters.....	24
5.1.5 Microbial community composition.....	26
5.2 OSL Flooding Experiments.....	31
5.3 OSL – Basin Intermittent Flooding Experiments.....	34
5.4 Flume Experiments.....	35
6 Scaling analysis.....	40
7 Key Findings.....	46
7.1 Hot spots and Hot Moments.....	46
7.1.1 Future Research.....	47
7.2 Use of Predictive Equations.....	47
7.2.1 Limitations.....	47
8 Recommendations.....	48
9 References.....	49

## Summary

The goal of this project was to identify the environmental drivers of microbial denitrification hot spots and hot moments in Minnesota's agricultural landscape, specifically in channels and floodzones (areas that are intermittently flooded with nitrate-laden water). We conducted a combination of laboratory experiments, outdoor experiments, and field monitoring to gain a mechanistic understanding of denitrification across a range of spatial scales, from microbial processes to field-scale processes. From this research, several drivers were found that increased denitrification and could be applied towards nitrate removal management strategies. These strategies include targeting areas with low-organic sediment and amending the sediment with a carbon source, modifying ditch or channel geometry to enhance connectivity with a floodplain, and manipulating water flow in ditches or channels. Results from this study indicated that periodic inundation increased denitrification rates, and that the timing and duration of flooding affects the microbial communities (abundance and diversity) in floodplain areas. Therefore, remediation strategies that create sites that periodically flood, and especially strategies that include constructed floodplains, have the potential to increase nitrate removal in agricultural ditches.

To evaluate potential management strategies for nitrate removal, predictive equations were developed and tested to predict relative denitrification rates in channels and floodplains. The in-channel equation was tested across two years of field data collection and compared well to previous research. The effect of inundation history on floodplain denitrification, however, limits the use of the floodplain equation, as the equation did not perform well across a dry and wet year. The temporal variability of denitrification rates and microbial communities in intermittently flooded areas needs to be better understood to accurately predict relative denitrification rates in floodplains across space and time.

## **Acknowledgements**

This report was compiled with input from all members of the research team. Ping Wang, Jacques Finlay, Martin du Suire, Kurt Spokas, Sandy Brovold, Shelly Rorer, and Christopher Staley provided laboratory assistance. The following undergraduate students assisted in field and experimental data collection and analysis:

- Chloe Winterhalter
- Noah Slocum
- Jesse Cutter
- Emily Jewell
- Victor French
- India Woodruff
- Aileen Zebrowski
- Rena Weis

This project was funded by the Clean Water Land and Legacy Amendment through the Minnesota Department of Agriculture's Clean Water Fund Research and Evaluation Program. Supplemental funding for undergraduate researchers was provided by the National Science Foundation (NSF) under the Research Experience for Undergraduate (REU) program and by the University of Minnesota Undergraduate Research Opportunity Program (UROP).

## 1 Background

Anthropogenic activities in the past century have greatly altered the global nitrogen cycle, especially in the agriculturally-dominated Midwestern United States, with severe consequences for human and aquatic health. The Haber-Bosch process has allowed for the modernization of agriculture through a process that fixes atmospheric nitrogen, producing readily available nitrogen fertilizer. Nitrogen recovery in crop plants is typically less than 50 percent globally (Fageria and Baligar, 2005), and thus approximately 25 percent of the nitrogen added to the biosphere is exported from rivers to oceans or inland basins (Mulholland et al., 2008). This inefficiency in crop nitrogen uptake and excess fertilizer applications to fields has caused negative human health effects (Powlson et al., 2008, Ward et al., 2010), and ecological consequences (Camargo and Alonso, 2006, Rabalais et al., 2007). Nitrogen loading to the Mississippi River from the agricultural region of the Midwestern United States is the predominate cause of the hypoxic zone in the Gulf of Mexico (Turner et al., 2006).

Due to these concerns, processes that remove nitrogen from water are of increasing interest. Denitrification and anammox, the oxidation of ammonium to nitrogen gas, are currently the only known natural microbiological pathways that remove substantial amounts of nitrogen from aquatic systems (Zhu et al., 2013). Complete denitrification is a stepwise microbial pathway that reduces soluble nitrate to inert nitrogen gas. Denitrification is primarily an anaerobic process, but has also been reported to occur in microaerophilic and aerobic systems, and is performed by a diverse range of bacteria and fungi (Zumft, 1997). The sequence of reducing transformations in the denitrification microbial pathway is shown in Figure 1. Denitrification functional genes have been identified that are responsible for each of the transformative steps and are, in stepwise order, *narG* or *napA*, which encode slightly different but equivalent nitrate reductase enzymes, *nirK* or *nirS*, which encode nitrite reductase, *cnorB* encoding nitric oxide reductase, and *nosZ* which encodes nitrous oxide reductase (Correa-Galeote et al., 2013, Barrett et al., 2013). Each of the enzymes encoded by these genes are inhibited by the presence of O<sub>2</sub> and require anoxic conditions to carry out their respective reactions (Guo et al., 2014). Incomplete denitrification results when nitrogen is not fully reduced to dinitrogen gas but instead to other oxidized forms of N including nitrous oxide (Braker and Conrad, 2011).

While some microbes are true denitrifiers and can individually complete the full reduction pathway from nitrate to N<sub>2</sub>, denitrification can also be considered a community process in that not all microbes possess all genes necessary for each step of denitrification. Denitrifiers are ubiquitous due to their metabolic flexibility and the fact that they are facultative anaerobes (Peralta et al., 2014). Despite resilient metabolic capabilities, denitrifiers only constitute approximately 5 percent of the total soil microbial community (Correa-Galeote et al., 2013).

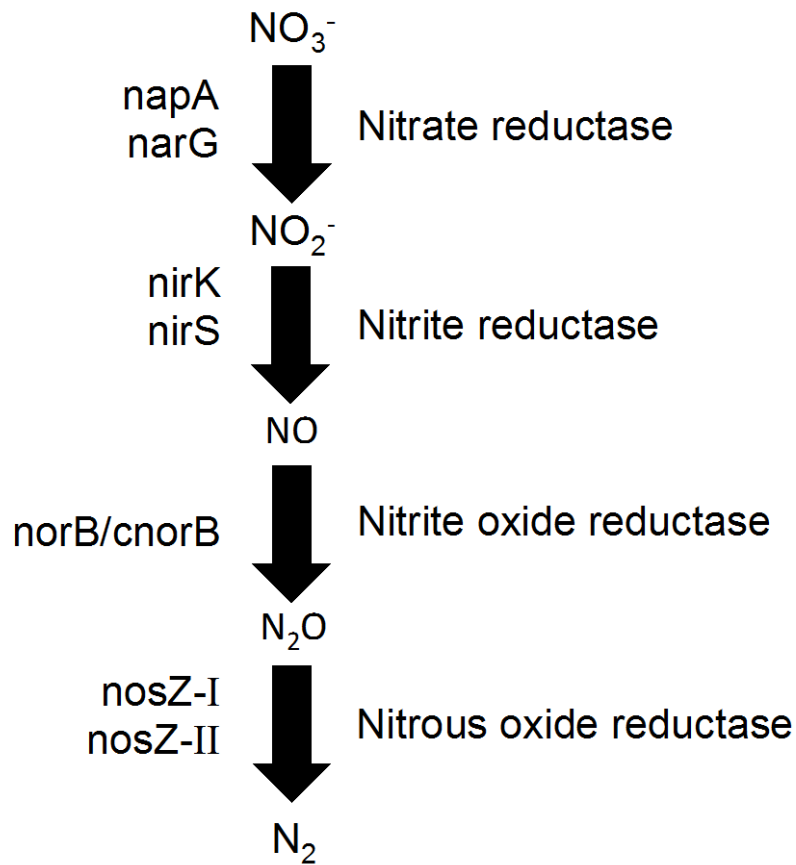


Figure 1. Flow chart depicting the stepwise pathway for complete denitrification. The functional gene and enzyme responsible for each transformation are shown to the right and to the left of the arrows, respectively. Note that in this study, the more universal molecular marker *NosZ3* replaced *nosZ-II*.

Isolated time periods and areas, termed hot moments and hot spots, respectively, frequently account for a large percentage of nitrate removal in aquatic ecosystems (McClain et al., 2003, O'Connor et al., 2006, Groffman et al., 2009, Guentzel et al., 2014). These hot spots and hot moments are formed by combinations of ideal environmental parameters and an established microbial community. Environmental parameters that affect denitrification rates include: organic carbon quality and concentration (Pinay et al., 2000, Perryman et al., 2011), sediment water content (Pinay et al., 2007), water velocity (Arnon et al., 2007), low sediment oxygen conditions, nitrate concentrations (Inwood et al., 2007), and floodplain location (Roley et al., 2012b, Roley et al., 2012a).

Headwater streams, agricultural ditches, and upland surface water features (wetlands) are important for nitrogen retention in Minnesota's agricultural landscape due to greater reactive surface areas (sediment water interface), residence times, and organic matter availability than downstream waterbodies. In addition, these features have the potential for greater hydrologic connectivity with intermittently flooded areas such as floodplains. Best management practices (BMPs) for nutrient removal such as detention/retention basins and compound channels (2-stage ditches with a floodplain) often rely on the assumption of greater nitrogen removal through

denitrification by increasing the area and time of contact between surface water and sediment microorganisms (Miller et al., 2012). To better predict the effect of surface water BMPs on microbial denitrification rates, this project sought to answer the fundamental question: *What physical and chemical processes determine the formation, performance, and disappearance of denitrification hot spots of microbial activity in surface water and adjacent transitional areas on the agricultural landscape?*

## 2 Project Goals

The goal of this project was to identify the drivers of microbial denitrification hot spots and hot moments in the Minnesota agricultural landscape, specifically in channels and floodzones (areas that are intermittently flooded with nitrate-laden water). Existing BMPS, such as installing flashboard risers, can be exploited to take advantage of ecosystem services that flooded soils provide in order to maximize denitrification, but questions remain as to what conditions optimize denitrification (e.g. carbon availability), and how much of the measured N loss is due to denitrification rather than short-term uptake or conversion to other forms of nitrogen. We conducted a combination of laboratory experiments, outdoor experiments, and field monitoring to gain a scientific understanding of the denitrification process across a range of spatial scales from microbial processes to field-scale processes (Figure 2).

Specifically, this project addressed the following objectives:

- 1) Identify the physical, chemical, and microbiological variables that drive enhanced denitrification rates in space and time (hot spots and hot moments) on the Minnesota agricultural landscape;
- 2) Explore the interaction of the driving physical, chemical, and microbiological variables within surface water engineered features on the agricultural landscape;
- 3) Develop a predictive methodology for denitrification rates in order to provide guidance for Minnesota water managers on how to design, operate, and maintain engineered surface water features to promote nitrogen removal.

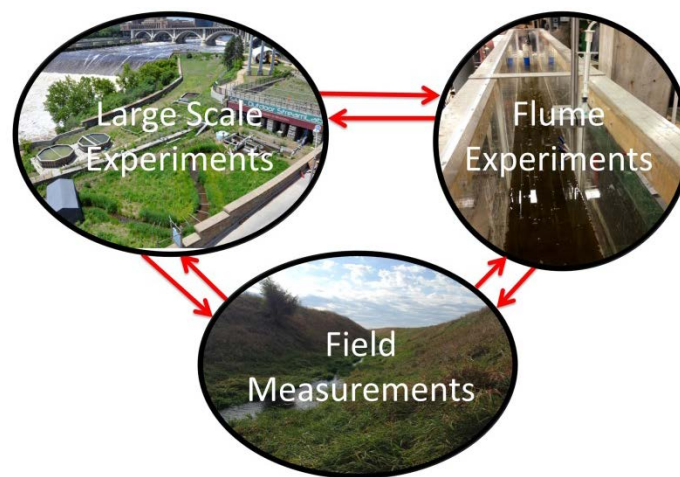


Figure 2. Experimental and data collection framework. A combination of laboratory, experimental outdoor facilities, and field data collection was used to examine the spatial and temporal variation in denitrification in MN agricultural surface waters and floodplains.

### 3 Experimental Setup

#### 3.1 Seven Mile Creek

Field data collection was conducted in the Seven Mile Creek watershed. The SMC watershed covers nearly 95.3 km<sup>2</sup> in Nicollet County and consists mainly of agricultural land (86% of the watershed). Most of the drainage entering the creek itself comes from constructed ditches and tile systems. The drainage ditches within the watershed have intermittent flow and often do not contribute water to the creek after July. This watershed was selected because SMC: 1) is primarily agricultural landuse; 2) has very high nitrate concentrations (>20 mg/L is typical for Spring months); and 3) has been previously studied by the research team (Sadowsky et al., 2010, O'Connor et al., 2006, Guentzel et al., 2014). Three sites were selected within the SMC watershed (Figure 3). Sampling sites were selected at locations previously monitored by the Minnesota Department of Agriculture (MDA) and Minnesota Pollution Control Agency (MPCA). Two agricultural ditch sites (SMC-1 and SMC-2) and a site within a non-ditched stretch of SMC (SMC-3) were visited in 2014 (June, August and September) and 2015 (May, June, July, August, and early November). Sediment samples were collected in the channel (IC), floodzone (FZ), and non-floodzone (NFZ) to analyze the relationships between environmental variables and denitrification in different hydrologic regimes (Figure 4). Measurements consisted of soil properties, soil water content, sediment microbiota, potential denitrification, aqueous nutrient concentrations, and flow characteristics as described in the methods section below.

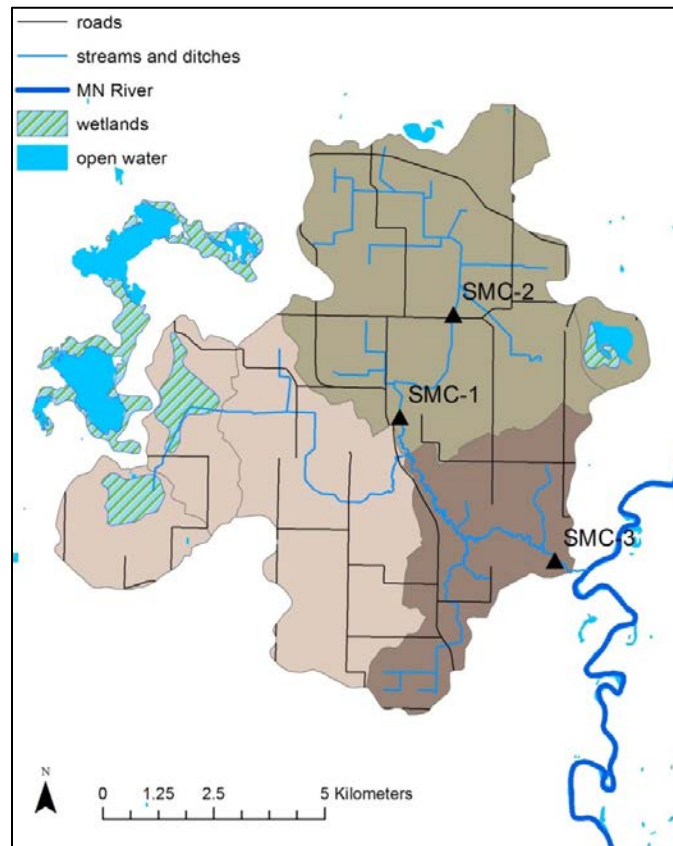


Figure 3. Map of Seven Mile Creek watershed with sites sampled in 2014 and 2015.

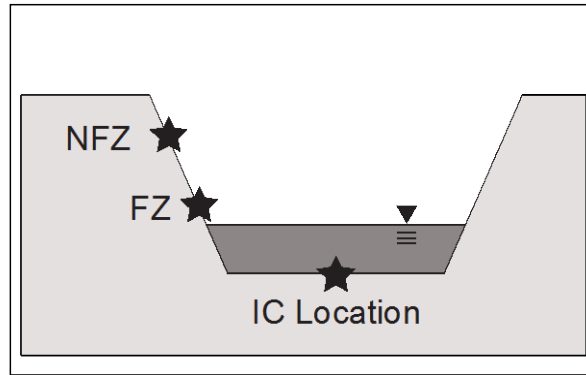


Figure 4. Illustration of sampling locations at each sampling site (IC = in-channel, FZ=flood-zone, NFZ=non-floodzone).

### 3.2 Outdoor StreamLab

The Outdoor StreamLab (OSL) is a unique large-scale research facility allowing field-scale experiments to occur in realistic outdoor settings under precise input controls (Figure 5). Two sets of experiments were conducted in the OSL. The first set of OSL experiments were conducted in the Riparian Basin of the OSL (Figure 5, right). The Riparian Basin of the OSL is a 40 m by 20 m experimental area currently configured into a vegetated floodplain with a small sand-bed meandering stream (average bankfull width 2.7 m average bankfull depth 0.3 m, sinuosity 1.3). The stream has been flowing year-round since June 19, 2008. The system is fed by Mississippi River water under valve control, thereby allowing precise control and monitoring of flow rates through the system. The bed sediment is mobile sand ( $D_{50} = 0.7$  mm and organic content  $< 2\%$ ). Sediment is metered into the stream inlet with a variable speed auger, captured at the downstream end, and recirculated for later feed. This outdoor laboratory enables controlled field-scale experiments on the physical, chemical, and biological interactions among a channel, its floodplain, and vegetation. A major advantage of this facility is that flooding can be controlled and is not dependent on natural climatic variability. Experiments in the OSL Riparian Basin examined the effect of individual flood events on in-channel and floodplain denitrification. Two floods were conducted in 2014 (June and July) at relatively high flow rates (920 L/s). These floods were repeated in 2015 (June and September) at lower flows (450 L/s), by backing up water on the floodplain. For each flood, the entire floodplain was inundated with at least 2 cm of water for the duration of the flood (approximately 4-5 hours). With the exception of the September 2015 flood, nitrate concentrations were equal to concentrations in Mississippi River water. Background nitrate concentrations were amended to approximately 1 mg/L in September 2015. Measurements consisted of soil properties, soil water content, sediment microbiota, potential denitrification, aqueous nutrient concentrations, and flow characteristics as described in the methods section below. In-channel and floodplain sediment samples were collected along a transect (Figure 6). Samples were collected immediately prior to each flood, immediately after, 1 day after the start of the flood and 3 days after the start of the flood to investigate the temporal variability of denitrification processes following a flood.



Figure 5. Layout of Outdoor StreamLab (OSL). A basin in the left photo was used to examine flooding duration and frequency in surface water storage features and the meandering channel on the right provides a field-scale channel with vegetated floodplain to investigate the impact of flooding duration and frequency in a flowing system.

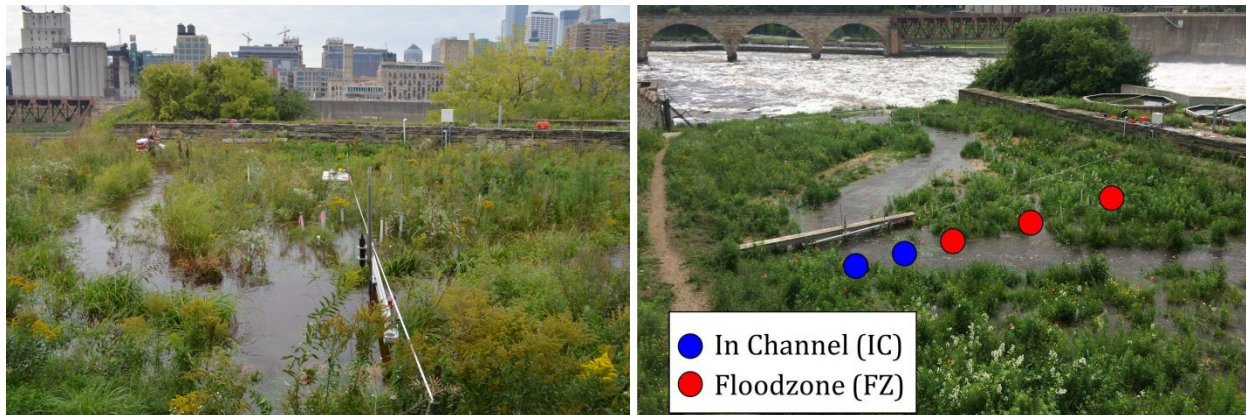


Figure 6. OSL during flooding experiments. (Left): September 2015 with acoustic Doppler velocimeter (ADV) set up, and (Right): sampling transect locations in the channel and on the floodplain.

The second set of OSL experiments (October-November, 2015) were designed to evaluate the influence of intermittent flooding on denitrification and utilized a controlled flooding basin. This basin was set up with three zones (similar to the field): always flooded (IC), floodzone (FZ) and non-floodzone (NFZ) as shown in Figure 7. Two types of sediment were tested in each zone: sandy sediment with very little organic matter, and organic sediment. Measurements consisted of soil properties, soil water content, sediment microbiota, microorganism DNA analysis, potential denitrification, and aqueous nutrient concentrations as described in the methods section below. Samples were collected after each change between flooding and non-flooding in the floodzone (Figure 8).

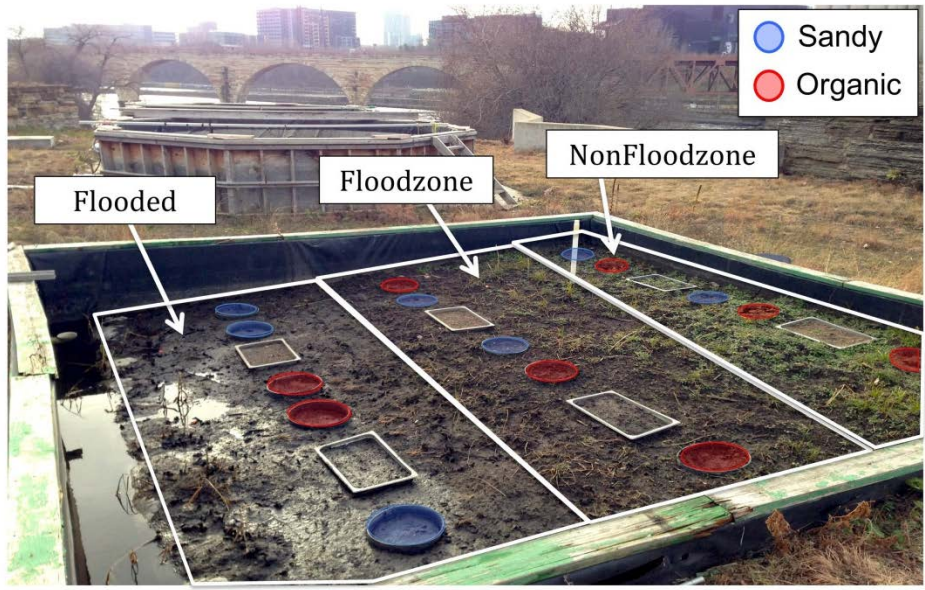


Figure 7. Schematic of the flooding basin showing the two sediment types and three flooding zones.

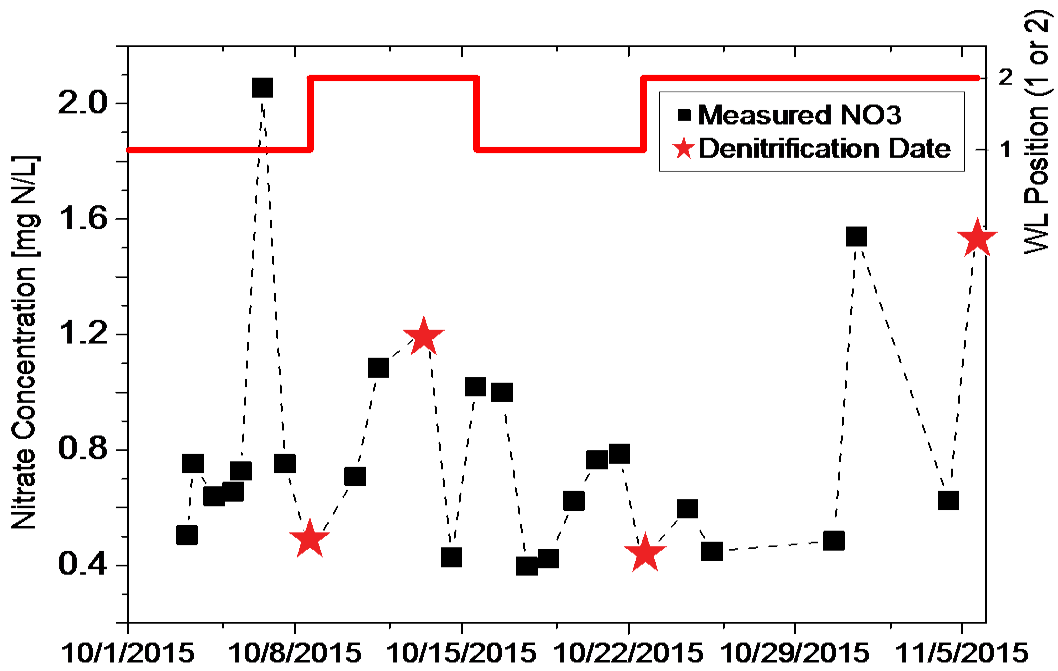


Figure 8. Timing of flood pulses during OSL basin experiment. Background nitrate concentrations are also shown. Sediment samples were collected before each step change between flooding to non-flooding (starred).

### **3.3 Flume**

Flume experiments were used to determine the effect of carbon type and water velocities on potential denitrification rates. Two carbon types, soybean meal and corn stover, were chosen as carbon amendments due to their prevalence in Southern Minnesota. A recirculating flume was used to determine the differences in potential denitrification rates between sediment, sediment augmented with ground corn stover, and sediment augmented with ground soybean meal under a control stagnant condition and four different velocities. Water and sediment for these experiments was collected in Seven Mile Creek.

The recirculating flume used is 0.2 m wide and 7.62 m long. Sediment depth was set to 5 cm because studies have shown that most denitrification occurs in the top 5 cm of sediment (Inwood et al., 2007). Silicone ice cube trays were used to divide each sample treatment and minimize disruption during sampling. Each tray contains six 5 x 5 x 5 cm compartments. In total, 40 trays in 3 colors (12 trays for each sediment type plus 2 trays at the beginning of the test section and 2 at the end) were placed in the flume in a randomly generated location. Each tray is 15 cm long, so the entire length of the sediment test section is 3 m. A Plexiglas false bottom that is 5 cm tall was placed upstream and downstream of the test section to maintain consistent water depth over the length of the flume. Flow straighteners were placed at the upstream end of the flume and foam was placed over the top of the flume to reduce evaporation.

Four velocities (2.5, 5, 7.5, and 10 cm/s) were used for flume experiments to determine the effect of water velocity on potential denitrification. Water was recirculated at each velocity for 2 weeks, after which the water was drained using a peristaltic pump and sediment was collected for denitrification potential and microbial analysis. Water depth was adjusted by adding spiked DI water at the beginning of each new velocity setting to maintain the 5 cm water depth over the test section as consistently as possible. Potassium nitrate was used to spike the DI water to bring initial flume water to 10 mg NO<sub>3</sub>-N/L at the beginning of each run. This concentration was selected since very high concentrations of nitrate have been shown in Seven Mile Creek and concentrations under 1 mg NO<sub>3</sub>-N/L have been shown to limit denitrification (Arango et al., 2007, Inwood et al., 2007). The spiked water was added to the drained field collected water, the flume was refilled with this water before each new velocity run was conducted. During each run, horizontal and vertical velocity profiles were collected at three locations using an acoustic Doppler velocimeter (ADV) mounted to a computer controlled vertical profiling instrument carriage (Figure 9). Dissolved oxygen (DO), temperature, specific conductance, and pH were constantly monitored in the flume. DO profiles were collected at three locations using an oxygen microsensor fitted to the ADV stem to quantify anoxic conditions in the sediment. Daily water samples were also collected for nitrate analysis using to determine the nitrate flux over the duration of the run.

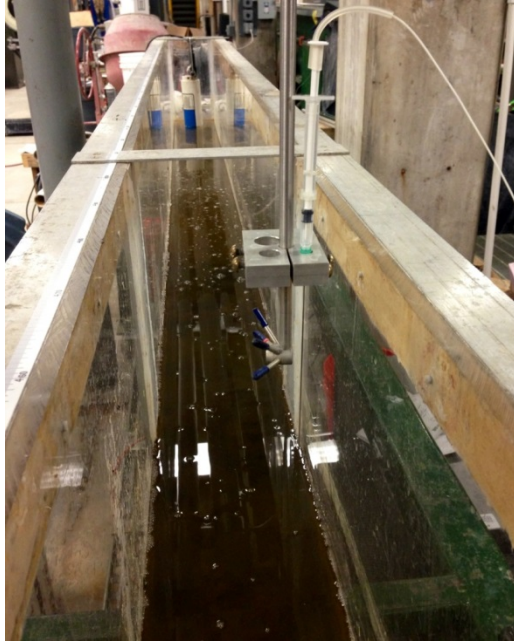


Figure 9. Flume Setup showing acoustic Doppler velocimeter (ADV) and dissolved oxygen needle for collection of oxygen microprofiles.

#### **4 Measurement Methods**

The following section describes specific methods for measurements described above. All water samples and sediment samples were collected in triplicate. Sediment cores collected in modified (top removed) 35 mL syringes were used to determine sediment properties. Cores for microbial measurements were collected using modified 5 mL syringes, and 60 mL syringes were used to collect sediment within the top 5 cm for denitrification rates. All triplicate sediment samples were collected within a 20 cm radius.

Table 1: Summary of data collection.

Site	Year	Dates	Parameters Measured					Description
			Sed.	Water	Microbio.	Flow	Other	
OSL	2014	Jun 23 Jul 8	OM MC $\rho_b$	$\text{NO}_3^-$ -N	DeN DEA DNA	3D IC 2D FZ	DO, pH, cond., temp. SM probes	~ 4 hour floods (920 L/s) samples collected: pre, post, 1 and 3 days post Locations: IC, FZ
	2015	Jun 25 Sep 25	OM MC $\rho_b$	$\text{NO}_3^-$ -N $\text{PO}_4^{3-}$ TDN DOC	DeN DEA DNA	3D IC 2D FZ	DO, pH, cond., temp.	~ 4 hour floods (450 L/s) with backwater samples collected: pre, post, 1 and 3 days post Locations: IC, FZ
SMC	2014	Jun 12 Aug 20 Oct 20	OM SM $\rho_b$	$\text{NO}_3^-$ -N	DeN DEA DNA Meta	2 or 3D IC	DO, pH, cond., temp.	Sites: SMC-1, SMC-2, SMC-3 Locations: IC, FZ, NFZ
	2015	May 15 Jun 15 Jul 15 Aug 18 Nov 9	OM MC $\rho_b$	$\text{NO}_3^-$ -N $\text{PO}_4^{3-}$ TDN DOC	DeN DEA DNA* Meta	2D IC	DO, pH, cond., temp.	Sites: SMC-1, SMC-2, SMC-3 Locations: IC, FZ, NFZ
Flume	2014	Feb-May	OM MC $\rho_b$	$\text{NO}_3^-$ -N	DeN DEA	3D profile	DO, pH, cond., temp.	3 carbon types (field, amended with soy meal, amended with corn stover) and 4 velocities
OSL- Basin	2015	Oct-Nov	OM MC $\rho_b$	$\text{NO}_3^-$ -N $\text{PO}_4^{3-}$ TDN DOC	DeN DEA	estimated	DO, pH, cond., temp.	Locations: IC, FZ, NFZ weekly fluctuation in water level for FZ Sediment: organic and sandy

OM = organic matter

MC = soil moisture content

$\rho_b$  = bulk density

TDN = total dissolved nitrogen

DOC = dissolved organic carbon

DeN = denitrification activity (site water)

DEA = denitrification potential (site water + nutrient amendments)

DNA = denitrification genes quantified using quantitative PCR

Meta = community composition using metagenomics

IC = in channel

FZ = floodzone

NFZ = non-floodzone

SMC = Seven Mile Creek

OSL = Outdoor StreamLab

**Sediment moisture content (MC)** was determined by using the gravimetric method (Black 1965; Gardner 1986). The volume and wet weight of the sediment cores were recorded, then dried for 24 hours at 110°C, or until the weight no longer changed, to determine the sediment dry weight. Moisture content (volumetric water content) was determined by subtracting the dry weight from the wet weight and normalizing by the sediment volume and a sediment depth of 5 cm. The spatial and temporal distribution of soil moisture was estimated for the 2014 OSL experiments by using a Soil Moisture Meter (TDR 100 Fieldscout Spectrum Technologies, Inc.).

**Sediment bulk density (BD)** was determined by dividing the dry weight by the volume of sediment (ASTM 2000).

**Sediment organic matter (OM)** Dried sediment was ground and sieved through a 2 mm screen, approximately 5 g was weighed into a crucible, the sediment was redried to remove the introduced moisture and reweighed, and heated to 550°C for 4 h (loss on ignition method) (Heiri et al., 2001). The ash-free dry mass (AFDM) was quantified by subtracting the ash weight from the dry weight, and the organic matter was determined by normalizing the AFDM in the same way as was done for moisture content.

**Nitrate concentration ( $\text{NO}_3^-$ -N)** All water samples were collected in triplicate. Water samples were filtered using pre-combusted 0.7  $\mu\text{m}$  Whatman GF/F filters and run on a Lachat QC800 Autoanalyzer (Hach Company) to determine nitrate concentrations ( $\text{NO}_3^-$  - N) using the cadmium reduction method (Kazemzadeh and Ensafi, 2001).

**Other water chemistry ( $\text{PO}_4^{3-}$ , TDN, DOC)** Water samples for dissolved organic carbon (DOC), total dissolved nitrogen (TDN), and phosphorus were filtered using pre-combusted GF/F filters. Samples for DOC and TDN were acidified with 2M HCl acid and concentration were determined using a TOC analyzer with a total N module (TOC-V CSH, Shimadzu) by high-temperature combustion with a Pt catalyst, followed by infrared gas analysis or chemoluminescence detection for DOC and TDN, respectively.

**Denitrification rate (DeN)** Denitrification rates of the sediment microbiota were determined using a modified acetylene block method (Groffman et al., 2009, Loken et al., 2016) using 40 g of field sediment, 40 mL of site-specific water, and 10 mg/L chloramphenicol to block de novo protein synthesis and to extend the linear period of  $\text{N}_2\text{O}$  accumulation (Tiedje et al., 1989). This method stops the conversion of nitrate to nitrogen gas at the production of  $\text{N}_2\text{O}$ , which is more easily measured than  $\text{N}_2$  due to atmospheric concentrations.  $\text{N}_2\text{O}$  concentrations were analyzed on a gas chromatograph (5890 series II, Hewlett-Packard) equipped with an electron capture detector and a headspace autosampler (Hewlett-Packard 7694).  $\text{N}_2\text{O}$  production was measured as the accumulation of  $\text{N}_2\text{O}$  over the incubation time and was corrected using the Bunsen solubility coefficient (Tiedje, 1982). Denitrification rates (in  $\text{mg-N/m}^2\text{h}$ ) were calculated as a function of bulk density and converted to an areal rate by assuming all denitrification occurs in the top 5 cm.

There are several potential limitations of this method, including not accounting for the activity from coupled nitrification-denitrification (Seitzinger et al., 1993), and acetylene may not completely inhibit the reduction of  $\text{N}_2\text{O}$  to  $\text{N}_2$  (Yu et al., 2010). However, for these experiments, this methodology was selected since it allows for a large number of samples to be run at a time, is appropriate when addressing the hot spot nature of denitrification (Groffman et al., 2006), and

rates have been shown to be similar to other methods when incubating over a short time period and with the addition of chloramphenicol (Bernot et al., 2003, Roley et al., 2012a).

**Potential denitrification rate (DEA)** Potential denitrification rates were determined using the same methodology as the DeN with the addition of nutrients (to measure with ability of soil microbiota to denitrify without nutrient limitation). Amendments included: nitrate (100 mg N/L as potassium nitrate), carbon (40 mg C/L as glucose), and phosphate (13.84 mg P/L as potassium dihydrogen phosphate).

**Evapotranspiration (ET)** was calculated for the floodzone and non-floodzone locations using a temperature-based method (Thornthwaite, 1948) to determine the potential evapotranspiration (PET), and ET was calculated from PET using the relative water content (the ratio of the difference in current water content and the permanent wilting point to the difference in the field capacity of the soil and the permanent wilting point) (Thornthwaite, 1948, Dingman, 2008). Weather data from the Mankato, Minnesota airport (weather station 56001, approximately 20 km away from the field site), were used for field weather conditions.

**Shear velocity ( $u^*$ )** was calculated by collecting velocities at several depths and using the logarithmic relationship between the time-averaged velocities and water depths (Biron et al., 2004). In situations where flow was either too slow or the logarithmic relationship was not evident, shear velocity was assumed to be 10 percent of the depth-averaged velocity. Water velocity measurements were obtained using an acoustic Doppler velocimeter (ADV). Two-dimensional velocity measurements were collected with a Sontek Flowtracker including most measurements in the field and on the floodplain in the OSL. In the flume and in the OSL channel, three-dimensional velocity measurements were collected using a Nortek Vectrino.

**Water quality parameters** including water temperature, pH, specific conductance, and dissolved oxygen (DO) were collected using a Hydrolab Series 5 Datasonde (Hach Company).

**Dissolved oxygen (DO) profiles** were collected in the flume experiments by attaching a dissolved oxygen (DO) micro sensor (PreSense) to the Vectrino ADV. For the flume experiments, this instrumentation was attached to a computer controlled instrumentation carriage.

## **4.1 Microbial Measurements**

### **4.1.1 Gene abundances (DNA)**

Quantitative PCR (qPCR) methods were used to determine the abundances of genes for each step in the denitrification pathway, *norB*, *narG*, *nirS*, *nirK*, *nosZ1*, and *nosZ3*. Total bacterial abundance was measured using the universal v4 region of 16S rRNA gene which covers eubacteria and archaea. MoBio PowerSoil DNA Isolation Kit (MoBio, Carlsbad, CA) was used to extract DNA from 500 mg of site sediment. DNA concentrations were measured on a Qubit 2.0 fluorometer (Life Technologies), and quantitative PCR (qPCR) was used to determine the concentration of each gene in sediment samples. The qPCR analysis was performed on a Roche Light Cycler 480 Real Time PCR (Roche Life Sciences, Indianapolis, IN) or an Applied Biosystems StepOnePlus Real-Time PCR System. The specific primers used are shown in Table 2.

Table 2. qPCR specifications for each denitrification gene.

Gene Name	Primer Set	qPCR Specifications	PCR/qPCR protocol	Ref.
<i>BAC515F</i> (16S rDNA)	U515F U806R	0.8 µl each primer 10 <sup>-4</sup> dilutions	(95°C:30s, 50°C:30s, 72°C:30s) x40	(P.Wang and M.Sadowsky, not published)
<i>cnorBB</i>	cnorB-BF cnorB-BR	0.8 µl each primer 50 ng BSA	(95°C:30s, 60°C:30s, 72°C:30s) x46	(C. E. Dandie et al. 2007)
<i>narG</i>	narG_1960m2fE narG_2050m2R	0.5 µl each primer	(95°C:15s, 58°C:30s, 72°C:30s) x46	(López-Gutiérrez et al. 2004), (Kandeler et al. 2006)
<i>nirK</i>	nirK876F nirK1040R	0.5 µl each primer	(95°C:30s, 63°C → 58°C 1°C/cycle] :30s, 72°C:30s) x51	(Bru et al. 2011; Petersen et al. 2012)
<i>nirS</i>	m-cd3AF m-R3cd	2 µl each primer Plasmid standard	(95°C:30s, 63°C → 58°C [-1°C/cycle] :30s, 72°C:30s, 81°C:30s) x55	(Hallin and Lingren 1999; Kandeler et al. 2009)
<i>nosZ1</i>	nosZ_F nosZ_1622R	1.2 µl each primer 10 <sup>-2</sup> dilutions	(95°C:30s, 65°C:30s, 72°C:30s) x51	(Rosch, Mergel, and Bothe 2002)
<i>nosZ3</i>	nosZ2F nosZ2R	1.2 µl each primer 10 <sup>-2</sup> dilutions	(95°C:30s, 65°C → 60°C 1°C/cycle] :30s, 72°C:30s) x51	(Bru et al. 2011; Petersen et al. 2012)

Each gene was run on a separate qPCR plate and a new standard curve was created for each run. The template DNA of each gene for making standard curve was PCR-cloned, sequenced and synthesized as gBlock fragments (gBlock fragments were ordered from Integrated DNA Technologies, Inc., Coralville, Iowa). The standard curve was created using the average of the Ct (threshold cycle) values output from the qPCR machine plotted against the log of the copy number of the dilution. The Ct values represent the number of cycles it took to detect a real signal from the sample. The standard curves for each gene were generated so that the efficiency (slope of the line) was between 80 to 110%, with a slope of -3.32 corresponding to 100% efficiency (Figure 10). The melting curve shows the temperature at which the amplified fragment of DNA denatures, referred to as the T<sub>m</sub> value. The more similar the DNA sequences, the closer the T<sub>m</sub> values are (Figure 11). The *nosZ3* gene had differing melting curves (Figure 11, bottom) for the samples and were therefore sequenced and analyzed against a database to confirm that they were the correct gene despite varying sequences.

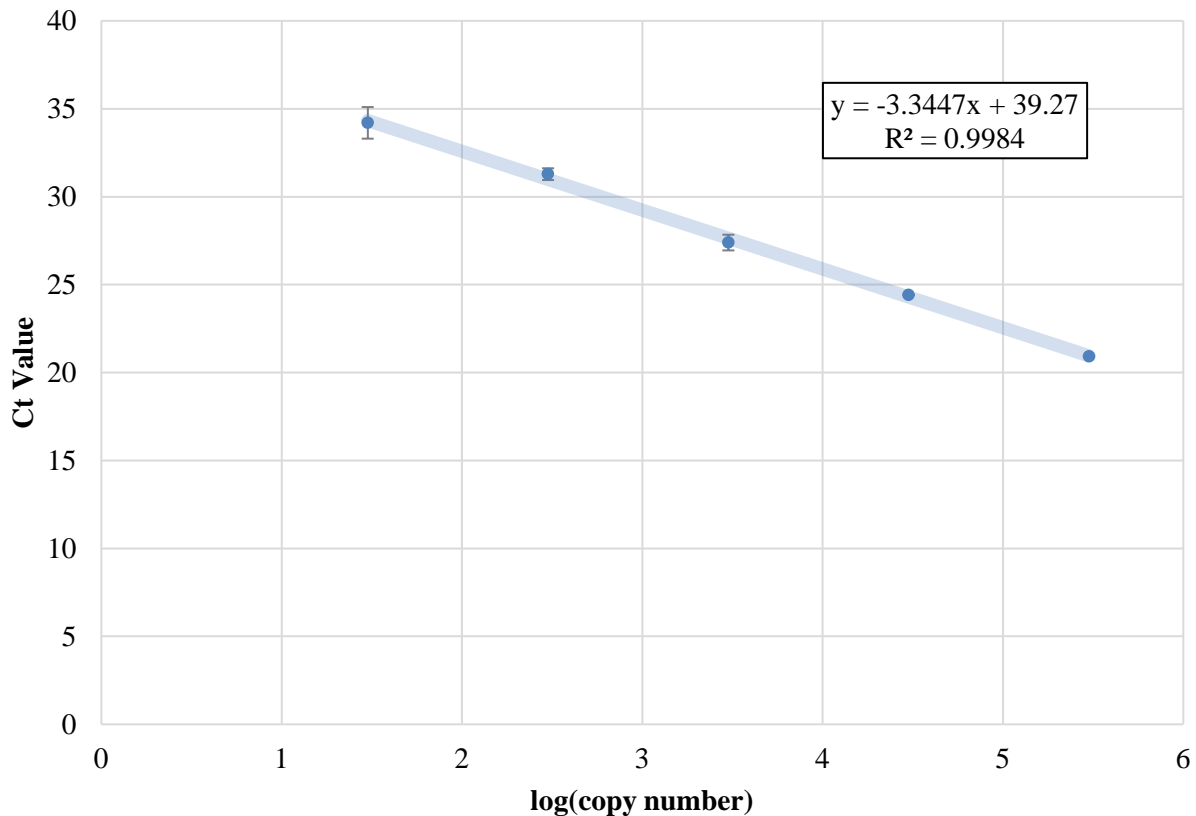


Figure 10. Example of standard curve: June 15, 2015 *narG*.

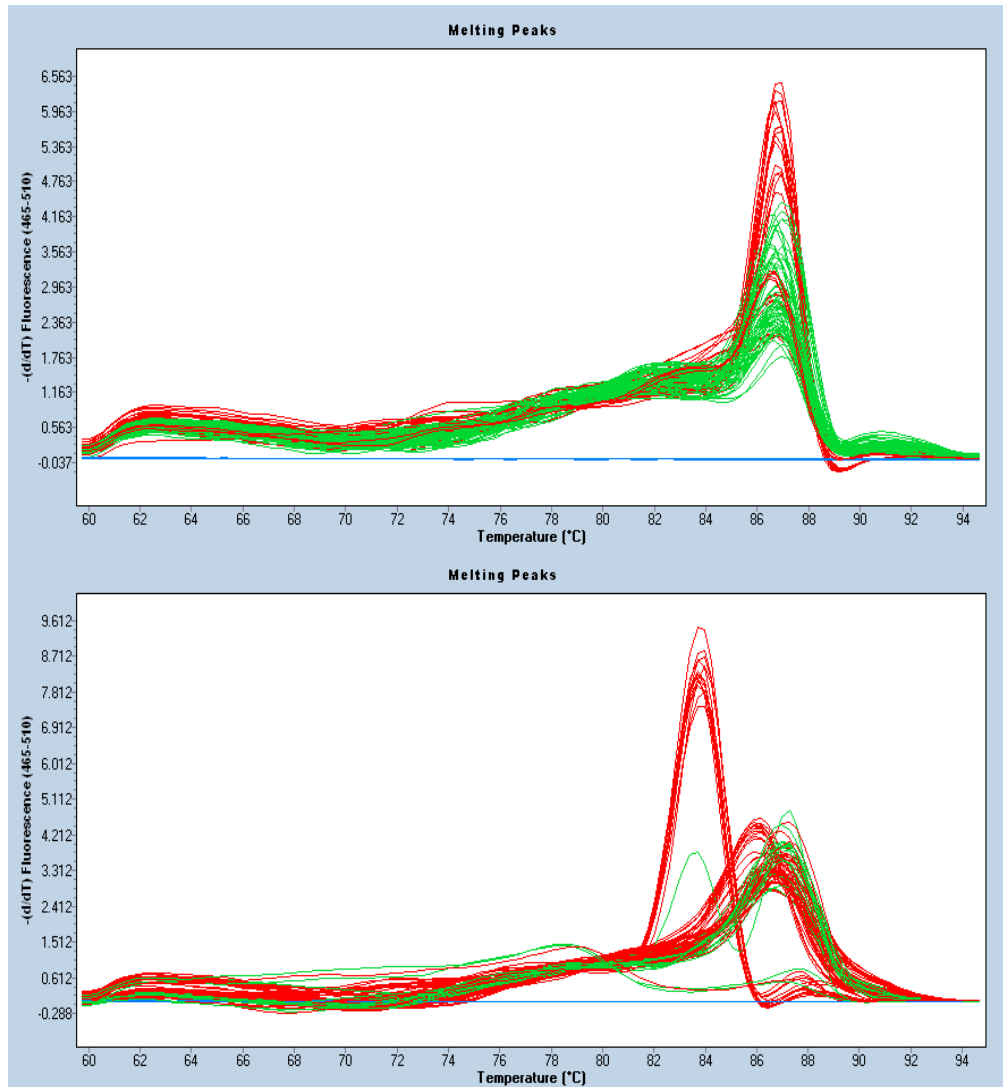


Figure 11. Examples of melting curves: Top: May 26, 2015 *cnorBB* melting curve from Roche Light Cycler 480. Single peak which is expected with samples from the same gene. Bottom: October 20, 2014 *nosZ3* melting curve from Roche Light Cycler 480. Example of a poor melting curve. Samples of varying  $T_m$  values were sequenced and compared against a database to confirm that they were the correct gene despite differences.

#### 4.1.2 Microbial community composition

Prokaryotic (archaeal and bacterial) communities from all samples were characterized by amplification and sequencing of the V4 hypervariable region of the 16S rRNA gene using the 515F/806R primer set (Caporaso et al., 2012). Sequencing was performed using the dual index method on Illumina platforms by the University of Minnesota Genomics Center. Sequence data were processed and analyzed as previously described, using mothur software (Staley et al., 2015; Schloss et al., 2009). Using this method, the relative abundances of operational taxonomic units (approximating species) were determined and could be classified to prokaryotic families to assess changes in community composition in each sample. Within-sample (alpha) and between-

sample (beta) diversities were assessed using the Shannon and Bray-Curtis dissimilarity indices, respectively, and ordination of Bray-Curtis distances were performed using principal coordinate analysis. Redundancy analyses and Spearman rank correlations were used to assess the relationships between prokaryotic community composition, physicochemical parameters, and denitrification gene abundances.

## 5 Results

### 5.1 Seven Mile Creek

#### 5.1.1 Environmental parameters and denitrification rates

Sampling in SMC spanned from summer to fall for both 2014 and 2015. The correlation between individual environmental variables, including temperature, bulk density, moisture content, organic matter, aqueous dissolved oxygen concentrations, stream shear velocity and depth, aqueous nitrate concentration, and DeN rates were compared. Air temperatures during sampling days are shown in Table 3, and the relationship between DeN rates and water temperature and dissolved oxygen are shown in Figures 12 and 13, respectively. Relationships between DeN rates and stream shear velocity and depth, aqueous nitrate concentration, bulk density, organic matter, and moisture content for in-channel sites are shown in Figure 14.

There were no direct correlations between air temperature and DeN at IC, FZ, or NFZ locations, or between water temperature and DeN at IC locations (Figure 12; (Lurndahl, 2016)). Dissolved oxygen was negatively correlated to DeN rates for all IC locations (Figure 13). DO was not measured in the sediment, but elevated levels of soil moisture can lead to limited oxygen delivery to soil microbes. For in-channel sites, DeN was only significantly correlated to water nitrate concentration and bulk density (Figure 14), although DeN generally increased with increasing organic matter. For non-channel sites, DeN was only significantly related to bulk density (Figure 15), but DeN generally increased with increasing organic matter and moisture content.

Table 3. Maximum daily temperatures on the dates of sampling, excluding November 2015. Air temperature maximums taken from the National Weather Service Reporting Station in St. Peter, MN and potential denitrification values for in-channel, floodzone, and non-floodzone samples across all dates.

	Sampling Date	Temperature (Celsius)
	June 12	28.3
2014	August 20	27.8
	October 20	28.3
	May 13	14.4
2015	June 15	29.4
	July 27	30.6
	August 17	26.7

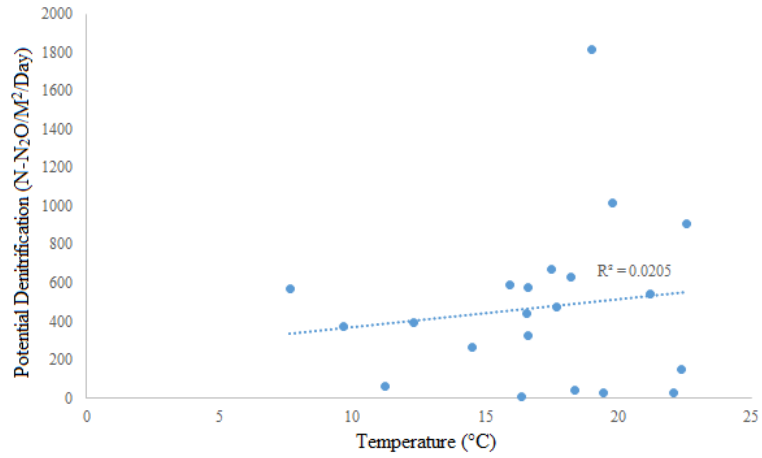


Figure 12. Averaged potential denitrification (DeN) rates and channel water temperatures for all sampling dates (Lurndahl, 2016).

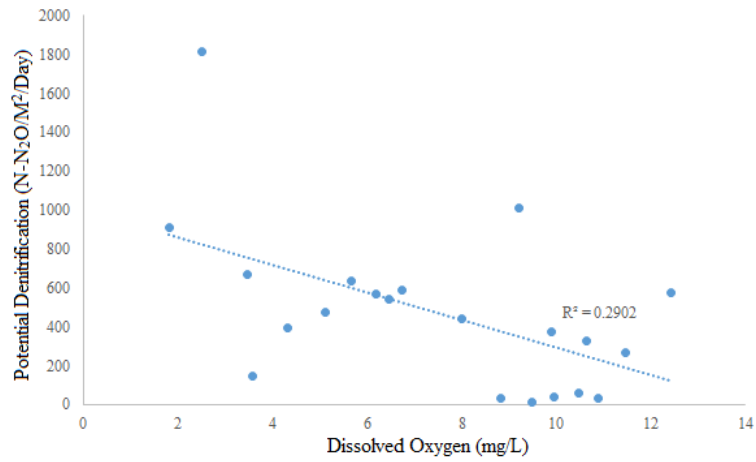


Figure 13. Averaged potential denitrification (DeN) rates and dissolved oxygen concentration of the channel water for all sampling dates (Lurndahl, 2016).

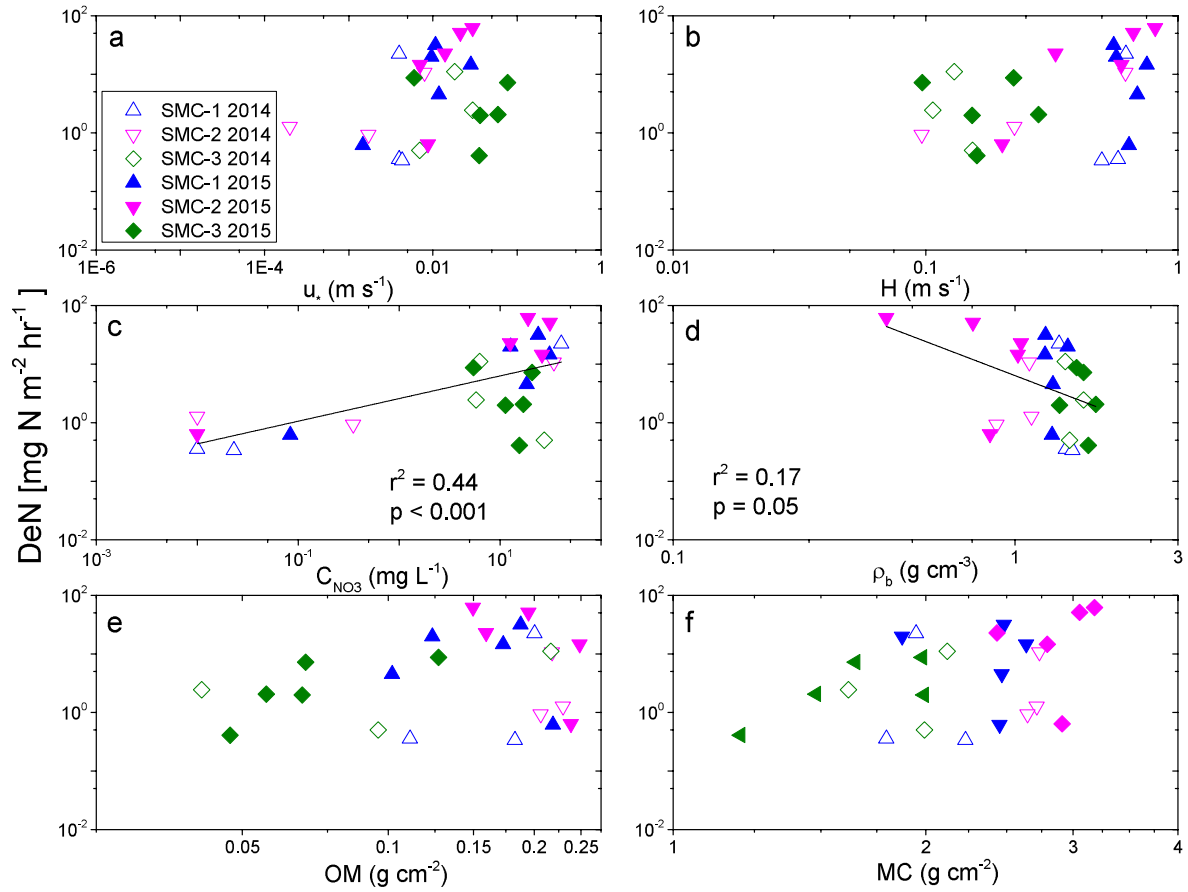


Figure 14. DeN as a function of individual parameters including (a) stream shear velocity ( $u_*$ ), (b) water depth ( $H$ ), (c) water nitrate concentration ( $C_{NO_3}$ ), (d) bulk density ( $\rho_b$ ), (e) organic matter (OM), and (f) sediment moisture content (MC) for in-channel locations in the SMC in 2014 and 2015.

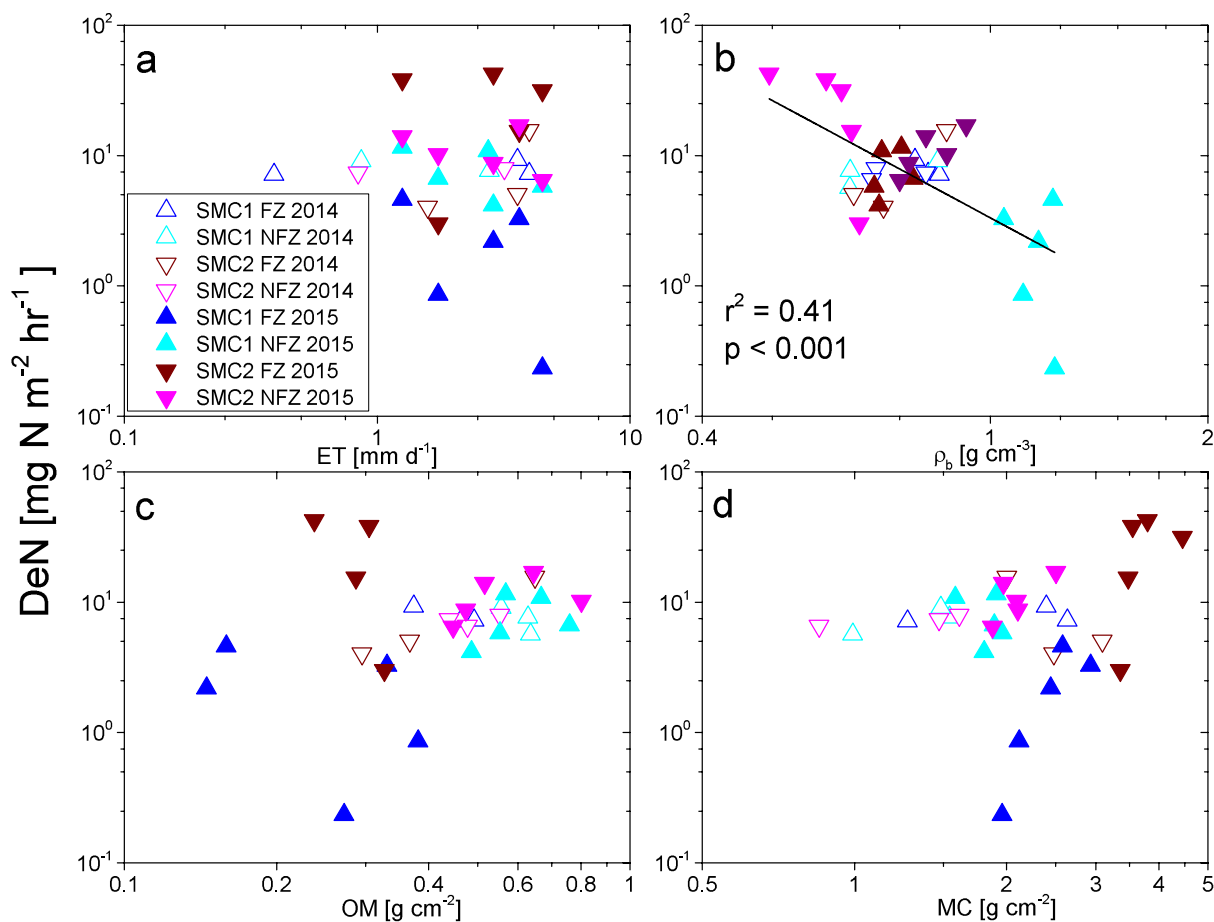


Figure 15. DeN as a function of individual parameters including (a) evapotranspiration (ET), (b) bulk density ( $\rho_b$ ), (c) organic matter (OM), and (d) sediment moisture content (MC) for locations in the floodzone and non-floodzone in the SMC in 2014 and 2015.

### 5.1.2 Denitrifying gene abundances

The total abundance of Prokaryotes (16S rRNA) and distribution of denitrifying gene abundances varied between IC, FZ and NFZ locations. Figure 16 shows the average percentage of each denitrifying gene as a percentage of the total abundance of denitrifiers, along with the average gene abundances of 16S rRNA in white triangles for SMC sites in 2014. This figure shows that the abundance of 16S rRNA is significantly greater at the floodzone locations. Non-floodzone locations had a different profile of denitrifying genes, specifically less *nirS* and more *narG*. The abundances of *nirS* gene are much greater in IC and FZ than in NFZ, and it is the major gene encoding the nitrite reductase. Conversely, the abundance of *nirK* gene in NFZ is higher than in IC and FZ, compared with the *nirS* gene. Gene data also showed that the SMC-3 site along with the non-floodzone location at SMC-2 had a much lower abundance of 16S rRNA than did the other sites.

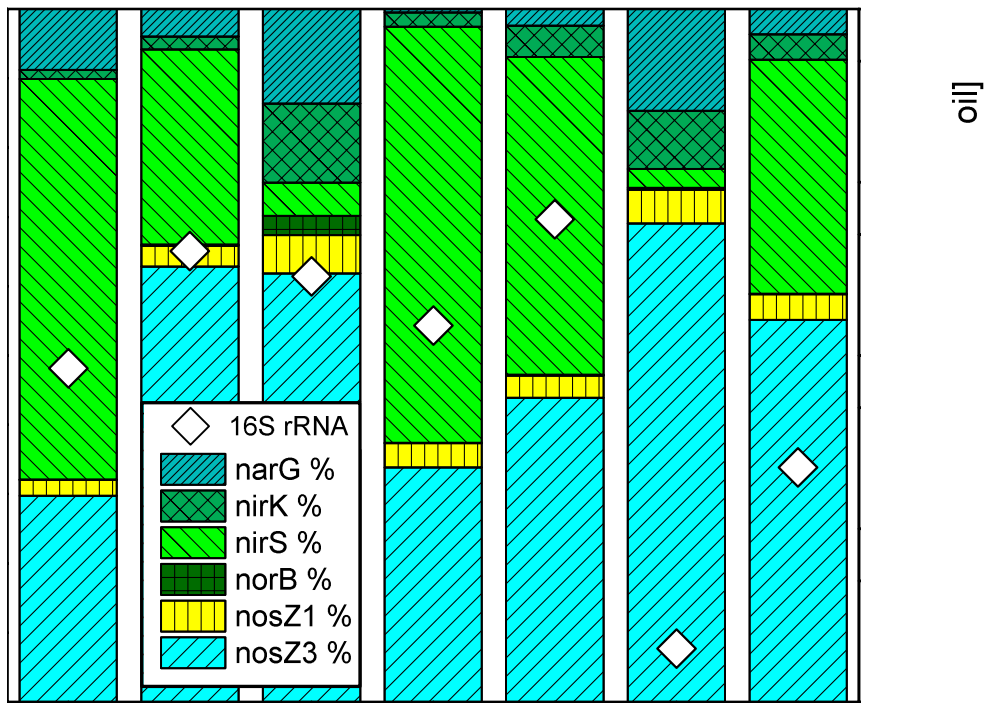


Figure 16. Average percentages of each denitrifying gene of the total abundance of denitrifiers, along with average 16S rRNA gene abundances (shown with white diamonds) at the field sites in the SMC watershed in 2014.

### 5.1.3 Seasonal DeN and DEA trends

As environmental variables changed across seasons (e.g. nitrate concentrations, flow rate and depth, temperature), denitrification rates showed seasonal variation. Figures 17 and Figure 18 show potential denitrification rates under site conditions (DeN) and non-limiting nutrient conditions (DEA) at all sites and locations for 2014 and 2015, respectively. In 2014, in-channel DeN rates were highest in June at both the SMC-1 and SMC-2 sites, with low rates in August and October. In August and October, in-channel rates increased when nutrients were added (comparing DeN to DEA). In 2015, in-channel rates were lowest in May and these rates increased when nutrients were added. For other dates in 2015 with low in-channel rates, these rates did not significantly increase when nutrients were added, indicating low potential for denitrification. August and October 2014 and May 2015 are the three dates when nitrate concentration at SMC-1 and SMC-2 were very low, possibly indicating nitrate limitation during these times (Figure 19). SMC-3 maintains higher nitrate concentration due to the groundwater inflow above this site. This is also supported by Figure 20, which shows the strong relationship between nitrate concentration and DeN rates. One point to note on this graph is the similarity of our line for the relationship between denitrification rates and nitrate concentration and the line from previous studies (Arango et al., 2007, Mahl et al., 2015).

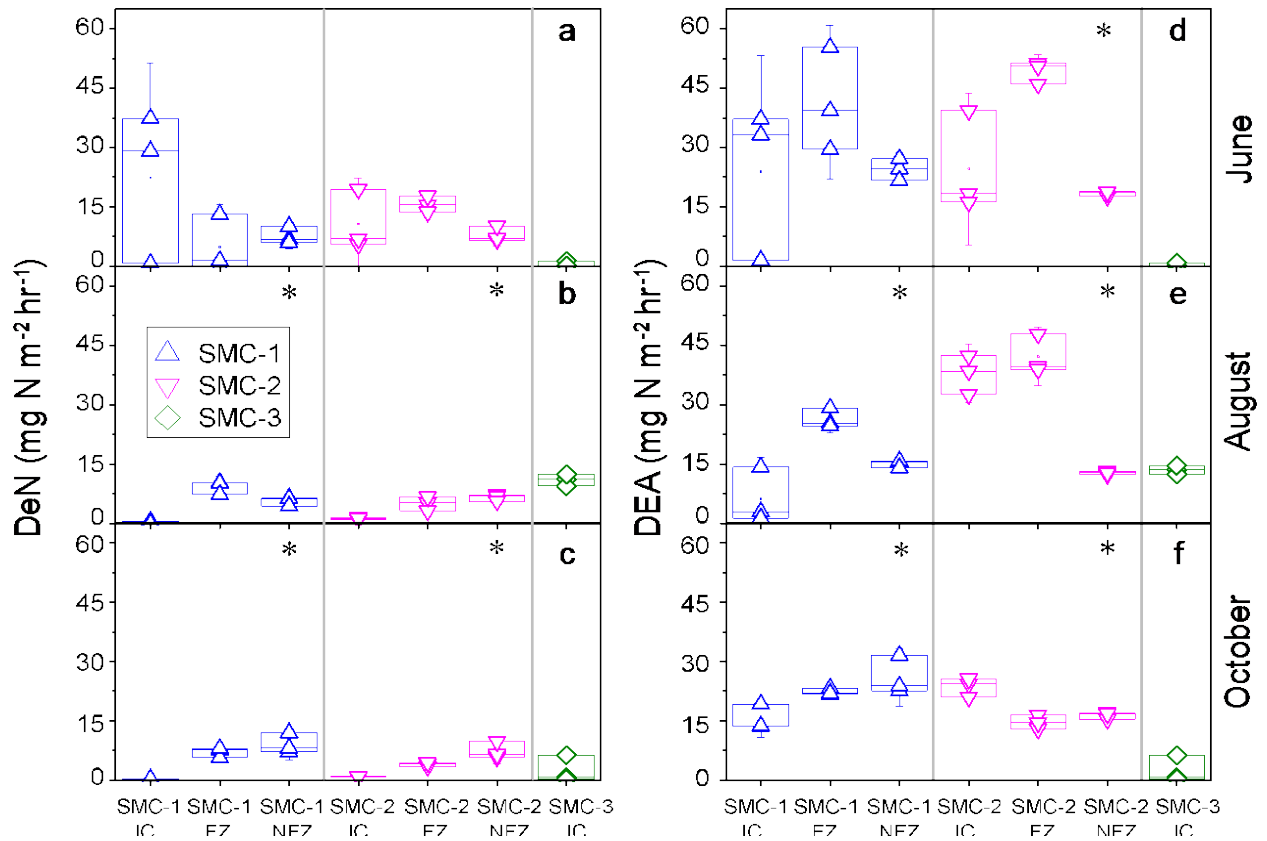


Figure 17. DeN rates for in-channel (IC), floodzone (FZ), and non-floodzone (NFZ) locations at the SMC-1, SMC-2, and SMC-3 sites on the (a) June, (b) August, and (c) October field sampling dates and DEA rates on the (d) June, (e) August, and (f) October field sampling dates. Asterisks represent field sites that had significantly ( $p < 0.05$ ) different denitrification rates by location (IC, FZ, and NFZ). Boxes represent the first and third quartile and whiskers represent  $\pm 1.5$  of the standard deviation.

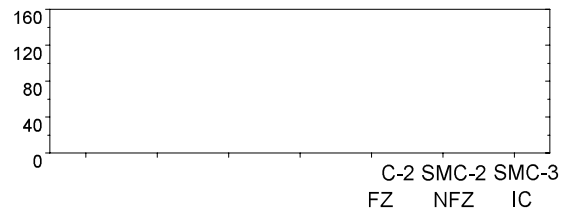


Figure 18. DeN rates for in-channel (IC), floodzone (FZ), and non-floodzone (NFZ) locations at the SMC-1, SMC-2, and SMC-3 sites on the (a) May, (b) June, (c) July, (d) August, and (e) November field sampling dates and DEA rates on the (f) May, (g) June, (h) July, (i) August, and (j) November field sampling dates. Boxes represent the first and third quartile and whiskers represent  $\pm 1.5$  of the standard deviation.

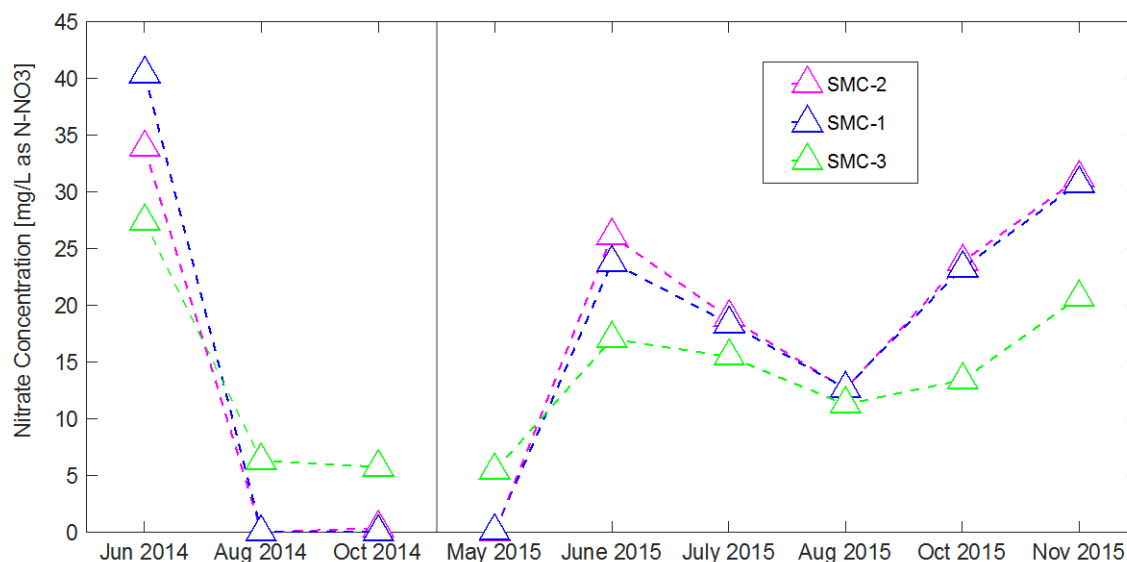


Figure 19. Nitrate concentrations at SMC-1, SMC-2 and SMC-3 for all sampling dates.

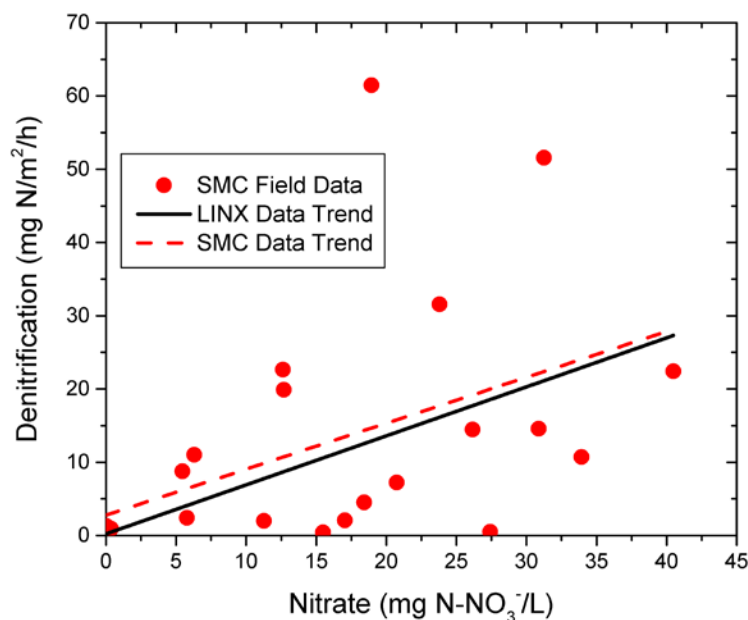


Figure 20. Relationship between nitrate concentrations and DeN rates from this study (red) and other studies (black line) (Arango et al., 2007, Mahl et al., 2015).

SMC-3 had low DeN and DEA across seasons and years with the exception of August 2014 and May 2015. In August, SMC-3 had a greater organic carbon content compared to the other sampling dates (3% compared to ~1%), probably due to the extensive flooding during the summer of 2014. In general, SMC-3 had very low organic carbon content and a sandy substrate. Our work from the OSL (discussed later in this report) suggests that sandy sediments may be limited in even establishing a bacterial community. This is also supported by the small difference

between DeN and DEA rates for SMC-3 and the relatively low bacterial abundance at SMC-3 (Figure 16).

Trends in the seasonal patterns for DeN and DEA rates suggest that site inundation and agricultural ditch geometry can affect nitrate removal rates. Ditch sites in this study had differing geometry with the SMC-2 site having an inset depositional floodplain at the floodzone location, whereas the SMC-1 site is trapezoidal with relatively steep banks. Sites with floodplain benches, like the floodzone location at SMC-2, provide benefits for nitrate removal through denitrification by increasing the bioreactive surface area and water residence time, slowing water velocities, reducing shear stress, and increasing in sediment deposition (Mahl et al., 2015, Roley et al., 2012b, Roley et al., 2012a). In 2014, the floodzone location within the depositional floodplain of SMC-2 had a higher DeN rate than the SMC-1 floodzone location in June; DEA rates were higher at the floodzone SMC-2 location compared to the floodzone location at SMC-1 in June and August. In 2015, the floodzone location at SMC-2 had higher DeN and DEA rates on every sampling date.

The DeN rates at the non-floodzone locations at both SMC-1 and SMC-2 remained similar across season and from 2014 to 2015. The effect of nutrient additions, comparing DeN to DEA, had a less pronounced effect on rates than it did for the in-channel and floodzone locations. This could suggest that these sites are more stable throughout the year and are less responsive to changing environmental conditions.

#### **5.1.4 Coupling between denitrifying gene abundances, denitrification rates, and environmental parameters**

Investigating the relationship between denitrifying gene abundances, denitrification rates, and environmental parameters addresses the question of whether increased denitrification rates in a landscape is a response where bacteria become more active (increased denitrification rate) or if bacterial abundances of denitrifiers increase. Tables 4-9 show significant correlations between gene abundances, denitrification rates, and environmental variables for each location and year. In both 2014 and 2015, there were many significant correlations between gene abundances, environmental parameters and denitrification rates for in-channel locations and very few for the non-floodzone locations. In 2014, there was some coupling between abundances, rates, and environmental parameters in the floodzone; however there were more significant relationships in 2015. In 2015, the floodzone location at SMC-2 was inundated for all but the May field sampling date, while in 2014 the floodzone location was never inundated on the sampling dates. Results suggest that the relationship between denitrification rates, gene abundances, and environmental parameters varies by hydrologic regime, and that the history of flooding can heavily influence denitrification behavior, particularly in floodzone locations.

Table 4. Correlations between gene copy number per gram dry soil, organic matter (OM), moisture content (MC), bulk density ( $\rho_b$ ), nitrate concentration ( $C_{NO_3}$ ), DeN, and DEA for in-channel (IC) locations in 2014 in Seven Mile Creek (SMC) represented with spearman  $\rho$  and the significance (p). Bolded numbers represent significant ( $p < 0.05$ ) correlations. Only significant correlations ( $p < 0.05$ ) are shown.

	16S rRNA		<i>norB</i>		<i>narG</i>		<i>nirS</i>		<i>nirK</i>		<i>nosZ1</i>		<i>nosZ3</i>	
	$\rho$	p	$\rho$	p	$\rho$	p	$\rho$	p	$\rho$	p	$\rho$	p	$\rho$	p
OM	.76	<.01	.55	<.01	-	-	.64	<.01	.68	<.01	.67	<.01	.69	<.01
MC	.70	<.01	.59	<.01	-	-	.71	<.01	.56	<.01	.60	<.01	.68	<.01
$\rho_b$	<b>-.73</b>	<.01	<b>-.53</b>	<.01	-	-	<b>-.63</b>	<.01	<b>-.45</b>	.02	<b>-.49</b>	.01	<b>-.63</b>	<.01
$C_{NO_3}$	-	-	<b>-.40</b>	.04	-	-	-	-	<b>-.41</b>	.03	-	-	-	-
DeN	.44	.02	-	-	-	-	-	-	-	-	-	-	-	-
DEA	.73	<.01	.58	<.01	-	-	.74	<.01	.50	<.01	.55	<.01	.60	<.01

Table 5. Correlations between gene copy number per gram dry soil, organic matter (OM), moisture content (MC), bulk density ( $\rho_b$ ), nitrate concentration ( $C_{NO_3}$ ), DeN, and DEA for in-channel (IC) locations in 2015 in Seven Mile Creek (SMC) represented with spearman  $\rho$  and the significance (p). Only significant correlations ( $p < 0.05$ ) are shown.

	16S rRNA		<i>norB</i>		<i>narG</i>		<i>nirS</i>		<i>nirK</i>		<i>nosZ1</i>		<i>nosZ3</i>	
	$\rho$	p	$\rho$	p	$\rho$	p								
OM	.76	<.01	.38	.01	.67	<.01	.48	<.01	.60	<.01	.41	<.01	.71	<.01
MC	.70	<.01	.51	<.01	.51	<.01	.50	<.01	.60	<.01	.61	<.01	.80	<.01
$\rho_b$	<b>-.63</b>	<.01	<b>-.49</b>	<.01	<b>-.38</b>	.01	<b>-.43</b>	<.01	<b>-.51</b>	<.01	<b>-.68</b>	<.01	<b>-.75</b>	<.01
$C_{NO_3}$	-	-	-	-	-	-	.30	.05	.56	<.01	.42	<.01	.43	<.01
DeN	.44	<.01	.44	<.01	-	-	-	-	.47	<.01	.69	<.01	.59	<.01
DEA	.65	<.01	.40	<.01	.41	<.01	.40	<.01	.47	<.01	.64	<.01	.68	<.01

Table 6. Correlations between gene copy number per gram dry soil, organic matter (OM), moisture content (MC), bulk density ( $\rho_b$ ), DeN, and DEA for floodzone (FZ) locations in 2014 in Seven Mile Creek (SMC) represented with spearman  $\rho$  and the significance (P). Only significant correlations ( $p < 0.05$ ) are shown.

	16S rRNA		<i>norB</i>		<i>narG</i>		<i>nirS</i>		<i>nirK</i>		<i>nosZ1</i>		<i>nosZ3</i>	
	$\rho$	p	$\rho$	p	$\rho$	p	$\rho$	p	$\rho$	p	$\rho$	p	$\rho$	p
OM	-	-	-	-	-	-	<b>-.68</b>	<.01	-	-	-	-	<b>-.54</b>	.02
MC	-	-	-	-	.57	.01	.62	<.01	.49	<.01	.67	<.01	-	-
$\rho_b$	-	-	-	-	-	-	<b>-.55</b>	.02	-	-	-	-	-	-
DeN	-	-	.56	.02	-	-	-	-	-	-	-	-	-	-
DEA	-	-	-	-	.49	.04	-	-	-	-	-	-	-	-

Table 7. Correlations between gene copy number per gram dry soil, organic matter (OM), moisture content (MC), bulk density ( $\rho_b$ ), DeN, and DEA for floodzone (FZ) locations in 2015 in Seven Mile Creek (SMC) represented with spearman  $\rho$  and the significance (P). Only significant correlations ( $p < 0.05$ ) are shown.

	16S rRNA		<i>norB</i>		<i>narG</i>		<i>nirS</i>		<i>nirK</i>		<i>nosZ1</i>		<i>nosZ3</i>	
	$\rho$	p	$\rho$	p	$\rho$	p	$\rho$	p	$\rho$	p	$\rho$	p	$\rho$	p
OM	-	-	-	-	-	-	.46	.02	-	-	-	-	.45	.02
MC	.55	<.01	.82	<.01	.63	<.01	.46	.01	.76	<.01	.78	<.01	.72	<.01
$\rho_b$	<b>-0.50</b>	<.01	<b>-0.82</b>	<.01	<b>-0.69</b>	<.01	<b>-0.42</b>	.02	<b>-0.76</b>	<.01	<b>-0.77</b>	<.01	<b>-0.80</b>	<.01
DeN	.52	<.01	.83	<.01	.70	<.01	.37	.05	.85	<.01	.76	<.01	.75	<.01
DEA	.48	<.01	.89	<.01	.71	<.01	.43	.02	.76	<.01	.82	<.01	.79	<.01

Table 8. Correlations between gene copy number per gram dry soil, organic matter (OM), moisture content (MC), bulk density ( $\rho_b$ ), DeN, and DEA for non-floodzone (NFZ) locations in 2014 in Seven Mile Creek (SMC) represented with spearman  $\rho$  and the significance (P). Only significant correlations ( $p < 0.05$ ) are shown.

	16S rRNA		<i>norB</i>		<i>narG</i>		<i>nirS</i>		<i>nirK</i>		<i>nosZ1</i>		<i>nosZ3</i>	
	$\rho$	p	$\rho$	p	$\rho$	p	$\rho$	p	P	p	$\rho$	p	$\rho$	p
OM	-	-	.57	.02	-	-	-	-	-	-	-	-	-	-
MC	-	-	-	-	-	-	-	-	<b>-0.64</b>	<.01	-	-	-	-
$\rho_b$	-	-	-	-	-	-	-	-	-	-	-	-	-	-
DeN	-	-	-	-	-	-	-	-	-	-	-	-	-	-
DEA	-	-	-	-	-	-	-	-	<b>-0.61</b>	<.01	-	-	-	-

Table 9. Correlations between gene copy number per gram dry soil, organic matter (OM), moisture content (MC), bulk density ( $\rho_b$ ), DeN, and DEA for non-floodzone (NFZ) locations in 2015 in Seven Mile Creek (SMC) represented with spearman  $\rho$  and the significance (P). Only significant correlations ( $p < 0.05$ ) are shown.

	16S rRNA		<i>norB</i>		<i>narG</i>		<i>nirS</i>		<i>nirK</i>		<i>nosZ1</i>		<i>nosZ3</i>	
	$\rho$	p	$\rho$	p	$\rho$	p	$\rho$	p	P	p	$\rho$	p	$\rho$	p
OM	-	-	-	-	-	-	-	-	-	-	-	-	-	-
MC	-	-	-	-	-	-	-	-	-	-	-	-	-	-
$\rho_b$	-	-	-	-	-	-	-	-	-	-	-	-	-	-
DeN	-	-	-	-	-	-	.38	.04	-	-	-	-	-	-
DEA	-	-	-	-	-	-	.47	<.01	-	-	-	-	-	-

### 5.1.5 Microbial community composition

Linkages between microbial community composition and denitrification were analyzed at each location using extracted DNA samples collected for determining denitrifying gene abundances. Site labeling in the below graphs is as follows: stream represents the in-channel location at the SMC-3 site, bank represents a location next to the stream at the SMC-3 site (only sampled in 2014), and channel, flooding zone, and non-flooding zone represents the in-channel, floodzone, and non-floodzone locations, respectively, at the SMC-1 and SMC-2 sites.

### Alpha diversity and community composition

A range of 385-8,160 OTUs (operational taxonomic units) was observed with a mean Good's coverage of  $96.3 \pm 0.3\%$ , among all samples. The Good's coverage provides information on the percent of total species represented in a sample, with a high number representing large coverage of the sample. Samples collected in 2014 had significantly lower alpha diversity, measured by the Shannon index, compared to samples collected in 2015 (Figure 21), meaning that 2014 samples had much less diversity in the community. In 2014, Shannon indices at SMC-1 and SMC-2 differed significantly by sample position where the diversity in the locations followed in-channel > floodzone > non-floodzone ( $P \leq 0.012$ ). However, the alpha diversity among the locations at SMC-3 did not vary by position ( $P = 0.975$ ) for all months sampled. In 2015, the difference in Shannon indices between in-channel and floodzone samples was not significant ( $P = 0.446$ ), but these samples had significantly greater alpha diversity than those from samples collected in the non-floodzone ( $P < 0.0001$ ).

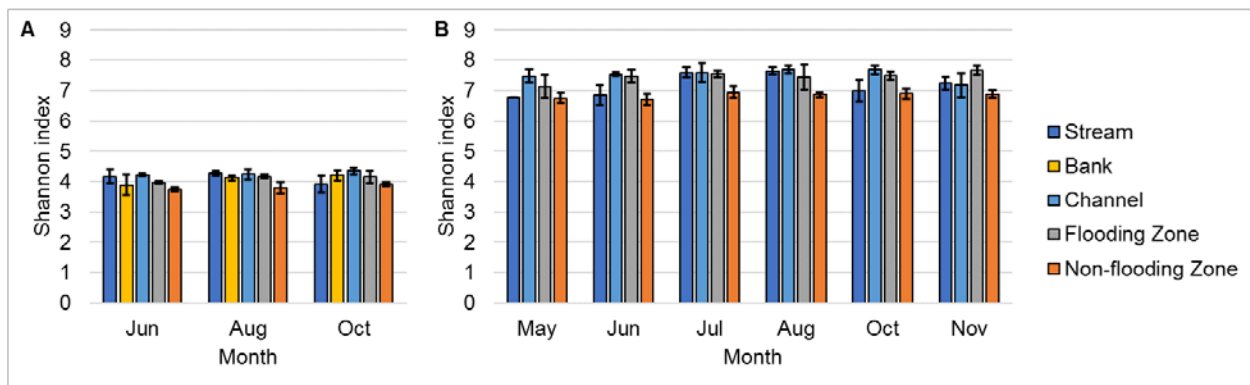


Figure 21. Shannon indices of samples grouped by locations. Shannon indices were averaged among all replicates at each month for samples collected in A) 2014 and B) 2015. Error bars reflect standard deviation.

During both years of sampling, communities from all sampling sites were predominantly comprised of members of the classes Actinobacteria,  $\alpha$ - and  $\beta$ -Proteobacteria, and Acidobacteria (Figure 22). Samples collected at the in-channel locations at the SMC-1, SMC-2, and SMC-3 sites tended to have greater abundances of  $\beta$ -Proteobacteria, while abundances of Actinobacteria,  $\alpha$ -Proteobacteria, and Acidobacteria were greater in the SMC-3 bank samples (2014) and those collected from the floodzone and non-floodzone locations at SMC-1 and SMC-2.

Among the families characterized, a greater relative abundance of *Burkholderiaceae* was observed among samples collected in 2014 than in 2015 (Figure 23), and the abundance of this family tended to decrease moving from in-channel to the floodzone and non-floodzone locations at SMC sites. Conversely, in 2015, greater relative abundances of less abundant families were observed in the in-channel locations, with increased abundance of the family *Anaerolineaceae*, relative to samples in the floodzone and non-floodzone locations (Figure 23B).

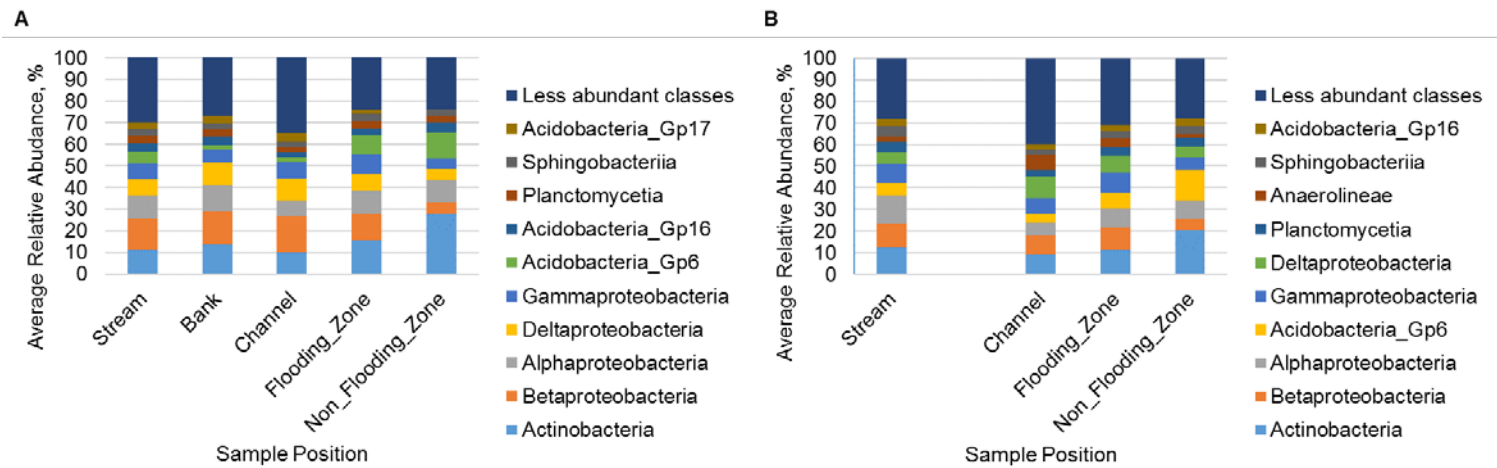


Figure 22. Distribution of abundant classes among samples grouped by position. Class abundances were averaged among all samples collected from a sampling position in A) 2014 and B) 2015.

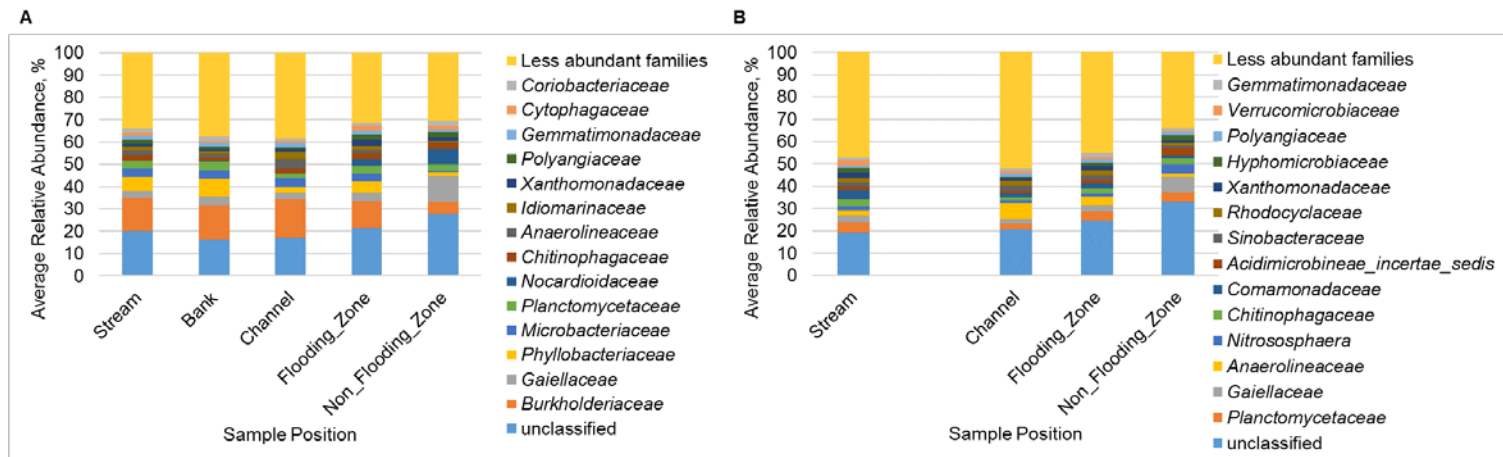


Figure 23. Distribution of abundant families among samples grouped by position. Class abundances were averaged among all samples collected from a sampling position in A) 2014 and B) 2015.

### **Beta diversity**

Differences in bacterial community composition among samples (beta diversity) were evaluated by analysis of similarity (ANOSIM), and communities differed significantly between sampling years ( $P < 0.001$ ). During both sampling years, beta diversity differences varied significantly as a result of sample location ( $P \leq 0.002$ ) but not the month of sampling ( $P = 0.102$  and  $0.740$  in 2014 and 2015, respectively). In 2014, community composition at SMC-1 and SMC-2 did not differ significantly ( $P = 0.025$ , Bonferroni-corrected  $\alpha = 0.017$ ), but community compositions differed significantly from those of samples collected at the SMC-3 site ( $P \leq 0.002$ ). In 2015, the community compositions in samples at each site were significantly different ( $P < 0.001$ ). During both years, sampling position showed a greater impact than sampling site on community differences (ANOSIM  $r = 0.71$  versus  $0.19$  for position and site in 2014 and  $r = 0.81$  versus  $0.27$  in 2015).

Ordination of Bray-Curtis dissimilarity matrices by principal coordinate analyses (PCoA) revealed clustering of samples primarily based on sample position (Figure 24). Furthermore, evaluation of sample clustering by analysis of molecular variance supported the results of ANOSIM.

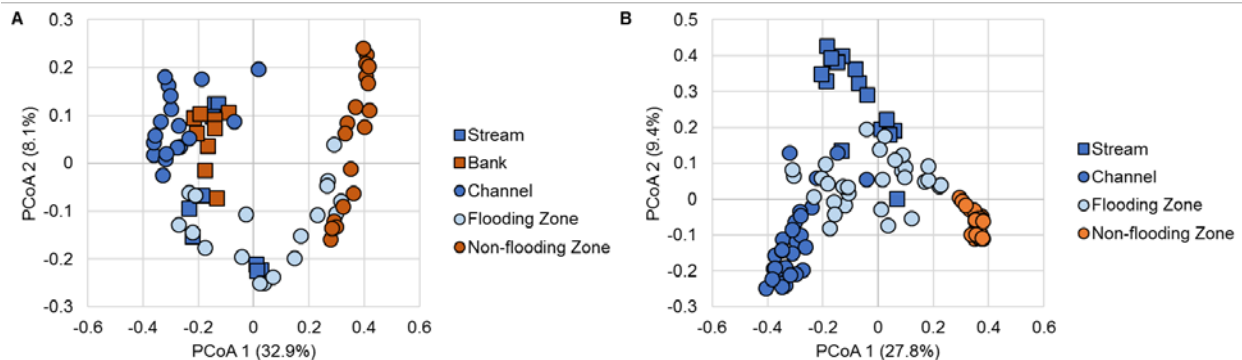


Figure 24. Principal coordinate analyses of Bray-Curtis dissimilarity matrices. Samples were collected in A) 2014 ( $r^2 = 0.72$ ) and B) 2015 ( $r^2 = 0.75$ ).

### **Relationship between bacterial community and denitrification**

Redundancy analysis was performed relating abundant bacterial families (present at a mean  $\geq 1.00\%$  of sequence reads), physicochemical parameters (nitrate, moisture, benthic organic matter, and bulk density), normalized abundances of denitrification genes (normalized to 16S rRNA gene copies), and other sample metadata (site, sampling position, and sampling month) from 2014 and 2015 samples (Figures 25 and 26). The relative abundances of several genes involved in denitrification were associated with abundances of bacterial families. Among associations observed in 2014 (Figure 25), normalized abundances of *nirS* were positively correlated with the abundances of *Burkholderiaceae* (Spearman's  $\rho = 0.500$ ,  $P = 0.005$ ) and *Idiomarinaceae* ( $\rho = 0.378$ ,  $P = 0.040$ ) and negatively correlated with abundances of *Bradyrhizobiaceae* ( $\rho = -0.577$ ,  $P = 0.001$ ). Normalized abundances of *NosZ3* were negatively correlated with abundances of *Gaiellaceae* ( $\rho = -0.450$ ,  $P = 0.013$ ), *Microbacteriaceae* ( $\rho = -0.433$ ,  $P = 0.018$ ), *Gemmatimonadaceae* ( $\rho = -0.641$ ,  $P < 0.001$ ), and *Nitrososphaera* ( $\rho = -0.380$ ,  $P = 0.039$ ). Few other associations were observed affecting the normalized abundance of denitrification genes based on their position near the origin in the redundancy analysis.

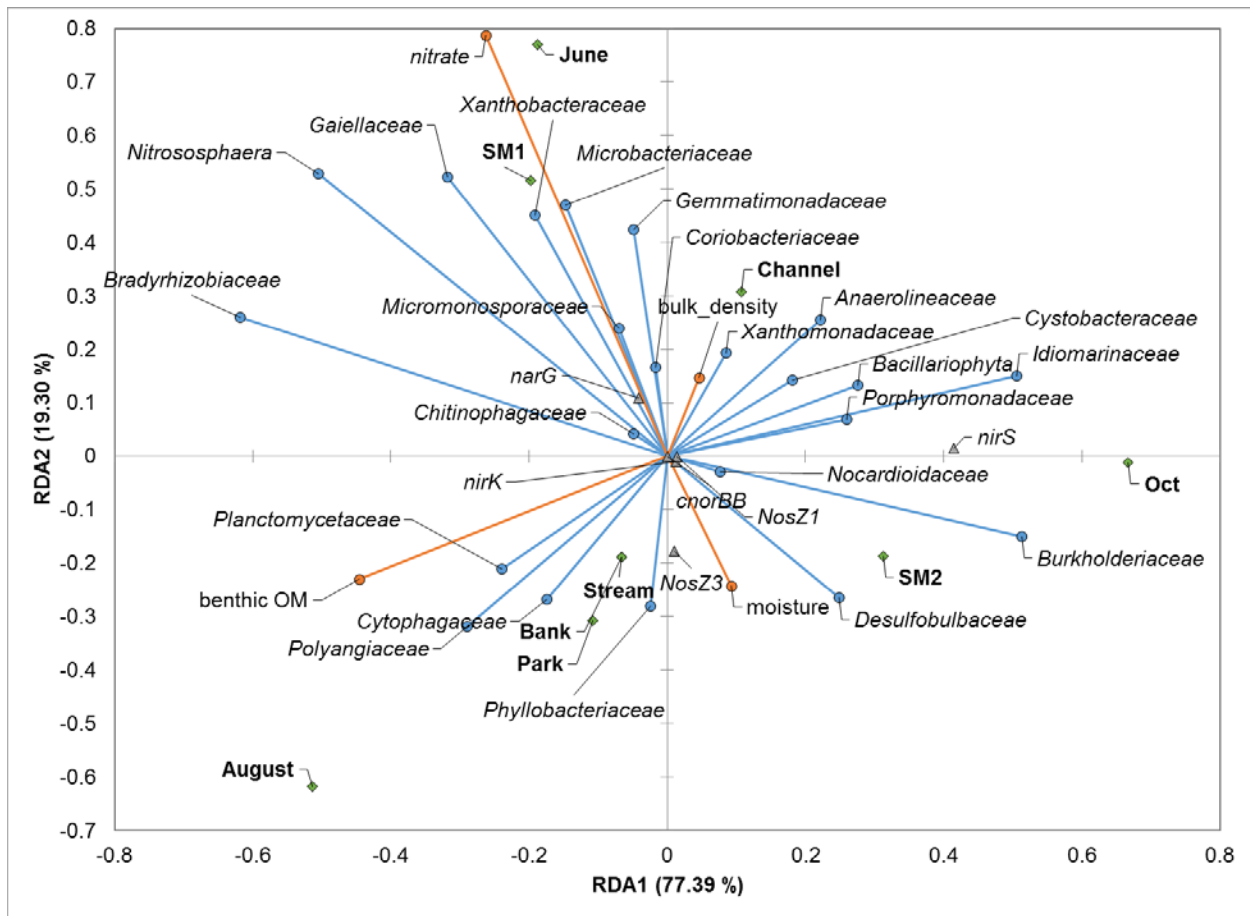


Figure 25. Redundancy analysis of 2014 bacterial families, denitrification genes, and other metadata. Bacterial families are shown in blue, physicochemical data are shown in orange, normalized abundances of denitrification genes are shown as gray triangles, and other metadata are shown as green squares.

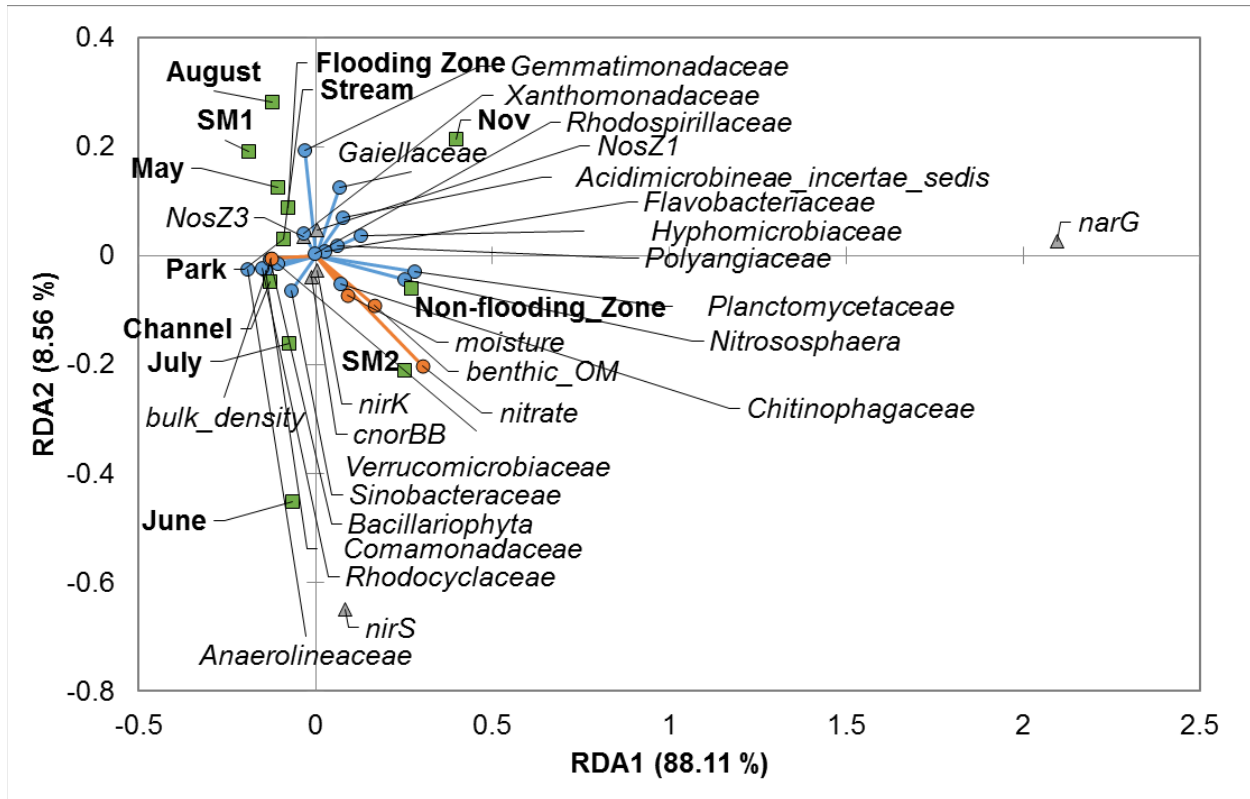


Figure 26. Redundancy analysis of 2015 bacterial families, denitrification genes, and other metadata. Bacterial families are shown in blue, physicochemical data are shown in orange, normalized abundances of denitrification genes are shown as gray triangles, and other metadata are shown as green squares.

Similar to relationships observed in 2014, abundances of few abundant bacterial families were associated with normalized abundances of denitrification genes (Figure 26). The normalized abundance of *narG* was positively correlated with abundances of *Anaerolineaceae* ( $\rho = 0.253$ ,  $P = 0.017$ ), *Sinobacteraceae* ( $\rho = 0.228$ ,  $P = 0.032$ ), and *Rhodocyclaceae* ( $\rho = 0.398$ ,  $P < 0.001$ ) and negatively correlated with abundances of *Gaiellaceae* ( $\rho = -0.380$ ,  $P < 0.001$ ), *Nitrososphaera* ( $\rho = -0.307$ ,  $P = 0.004$ ), and *Acidimicrobinae incertae sedis* ( $\rho = -0.436$ ,  $P < 0.001$ ). However, other relationships observed in the redundancy analysis were not significantly associated by Spearman correlation.

## 5.2 OSL Flooding Experiments

Four experimental floods were conducting in the Riparian Basin of the OSL, two in 2014 and two in 2015. The purpose of these experiments was to determine the effect of short-term flood events on denitrification rates and the microbial community. Figure 27 shows denitrification rates for the June and July flood for immediately before (0 hours), immediately after (5 hours), 1 day after (29 hours), and three days after (77 hours) the flood. Denitrification rates varied respect to sampling location (channel verses floodplain) for both the June and July flood, and denitrification rates were consistently higher at the floodplain sites than in-channel sites.

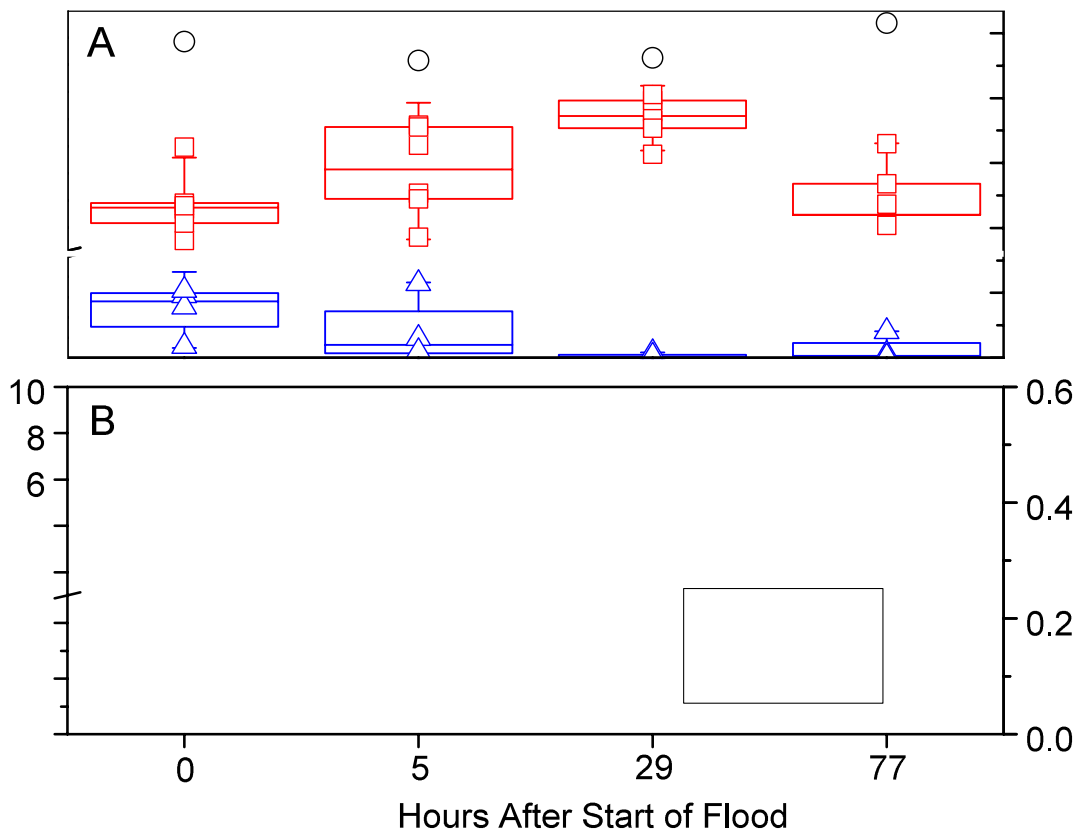


Figure 27. Nitrate concentrations of the Mississippi River water flowing through the experimental stream and denitrification rates at floodzone (FZ shown in red), and in-channel (IC, shown in blue) sites during the (A) June and (B) July floods. Boxes represent the first and third quartile and whiskers represent  $\pm 1.5$  of the standard deviation.

For both the June and July floods, denitrification rates at the in-channel sites decreased after flooding, however this difference was only significant ( $p=0.04$ ) for the June flood. During the 2014 flood events, shear stress in the channel was very high, which mobilized the sandy bed. Previous research has found that fast water velocities limit nitrate uptake (O'Connor and Hondzo, 2008, Alexander et al., 2009, Bukaveckas, 2007, O'Connor et al., 2012).

Floodplain denitrification rates significantly varied ( $p=0.001$ ) by sampling time (time after flood) during the June flood, but were independent of time during the July flood. For the June flood, denitrification rates at the floodplain sites increased up until 1 day after the flood, and then returned to pre-flood rates 3 days after the flood. Floodplain rates remained relatively constant for all sampling times during the July flood. The nitrate concentration of the Mississippi River water flowing through the experimental stream was much higher during the June flood (mean  $1 \text{ mg NO}_3\text{-N L}^{-1}$ ) than the July flood (mean  $0.5 \text{ mg NO}_3\text{-N L}^{-1}$ ). The increase seen in denitrification rates from the June flood may indicate the formation of hot moments from short duration flood events. The differences seen between the June and July may indicate a response limit for

bacteria, where flooding with water above this limit would increase denitrification due to a physiological response.

Total bacteria (16S rRNA concentrations) and the abundances of six denitrifying genes were quantified for the June and July floods using qPCR. Concentrations of the 16S rRNA gene copy number and five of the denitrifying genes immediately before, immediately after, and one day after the June flood are shown in Figure 28. Gene abundances for 16S rRNA, *narG*, and *nirK* significantly decreased at the in-channel and floodplain sites after the June flood, and *nosZ1* significantly decreased at the floodplain sites after the flood. Other gene abundances remained nearly constant during all sampling periods. For all genes, abundances in the sandy in-channel sites were much lower than those seen for the floodplain sites. Bacterial abundance results suggest that the observed increase in denitrification rates in the June flood event was likely due to higher physiological activity, as opposed to increasing microbial numbers.

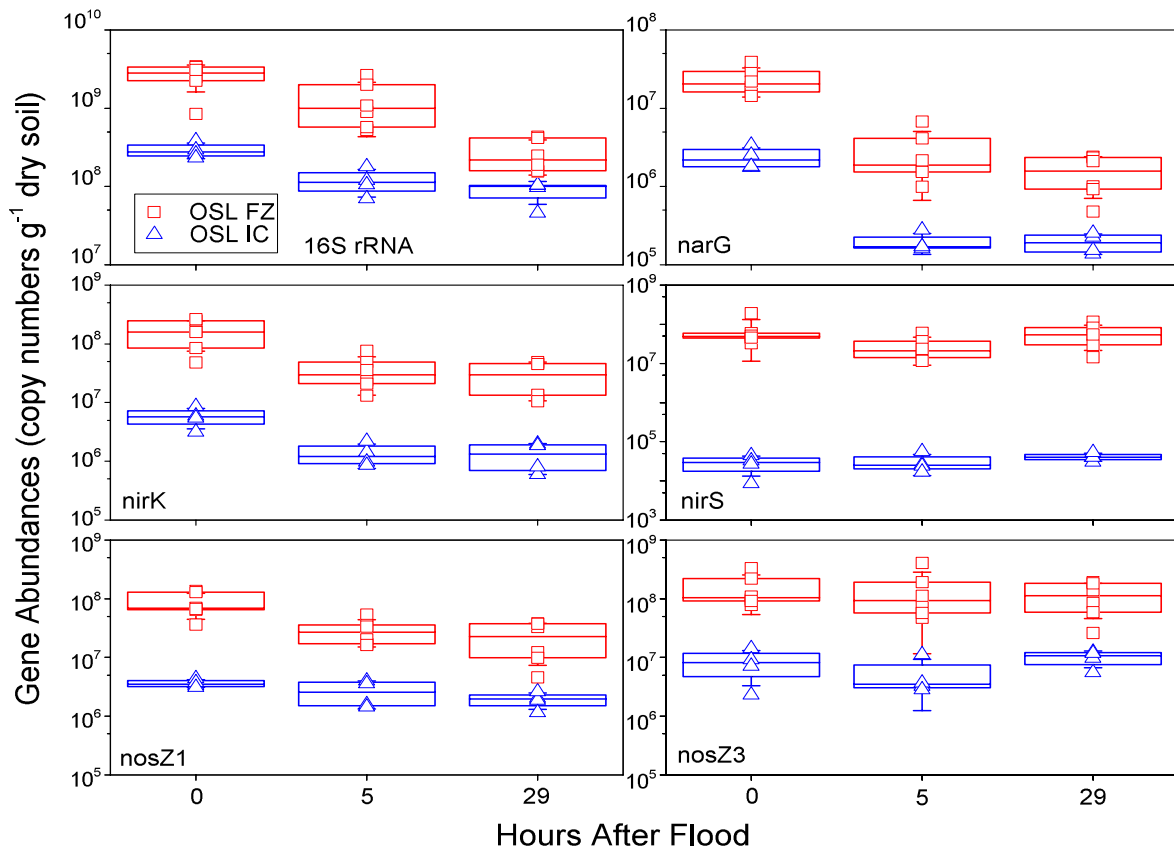


Figure 28. Gene abundances in copy numbers per gram of dry soil for (A) 16S rRNA, (B) *narG*, (C) *nirK*, (D) *nirS*, (E) *nosZ1*, and (F) *nosZ3* for the June flood in the experimental stream at floodzone sites (FZ, shown in red), and in-channel sites (IC, shown in blue). Boxes represent the first and third quartile and whiskers represent the standard deviation.

### **5.3 OSL – Basin Intermittent Flooding Experiments**

An experiment was conducted in the flooding basin of the OSL to determine the effect of intermittent flooding on denitrification. The flooding basin was divided into three hydrologic regimes (always flooded, periodically flooded, and never flooded) with two sediment types, a sandy sediment (organic matter of 1%) and an organic sediment (organic matter of 7%). The experiment was conducted for a month and the water level was maintained above the always flooded regime for the entirety of the experiment, raised and lowered over the periodically flooded regime in 1-week increments, and always kept below the never flooded regime.

Denitrification rates in the flooding basin experiment for the four sampling dates are shown in Figure 29. Overall, the rates for the organic sediment were higher than that of the sandy sediment, particularly at the floodzone location. The rates for the two sediment types also exhibited different patterns. Denitrification rates for the sandy sediment were greatest at the flooded location and decreased to the non-floodzone location, however only the October 15 sampling date was significantly different ( $p < 0.001$ ). Rates in the organic sediment were significantly greater at the floodzone location with similar rates at the flooded and non-floodzone location, except for the October 8 sampling date. At this date, however, the water level had not yet been raised to cover the floodzone location so a differential trend was expected. Results from the flooding basin suggest that the periodically inundated sites may represent denitrification hot spots.

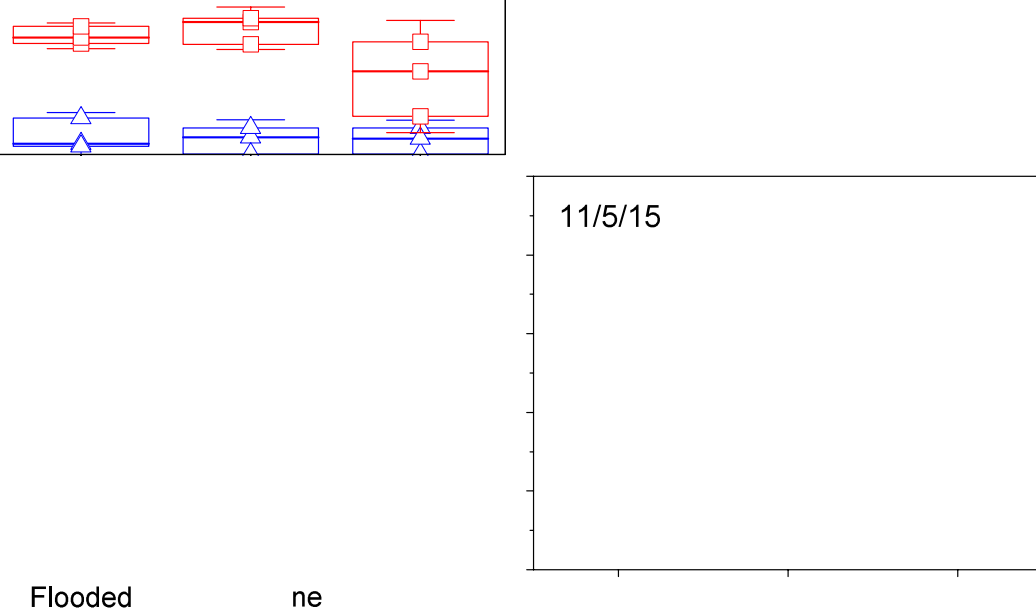


Figure 29. Denitrification rates for the organic (shown in red) and sandy sediments (shown in blue) on the (A) October 8 (water between the A-I and P-I interval), (B) October 15 (water between the P-I and N-I interval), (C) October 22 (water between the A-I and P-I interval), and (D) November 5 (water between the P-I and N-I interval) sampling dates. Boxes represent the first and third quartile and whiskers represent  $\pm 1.5$  of the standard deviation.

#### 5.4 Flume Experiments

Three sediment types and four velocities, along with a stagnant control condition, were tested in a flume at the St. Anthony Falls Laboratory to determine the effect of velocity and carbon amendments on denitrification. The flume results indicate an overall trend in increasing potential denitrification (DEA, non-limiting nutrient conditions) with increasing velocity (Figure 30). Due to the experimental design, this could also be attributed to the length of time the sediment had to establish a denitrifying community (the sediment at the higher velocity had been in the flume longer than at the slower velocities). From the results, soy amended sediment consistently had the highest rates, followed by amended corn. There was little difference between unamended and amended unaugmented (control) sediment, which was sediment as collected from Seven Mile Creek with no carbon amendments to the soil.

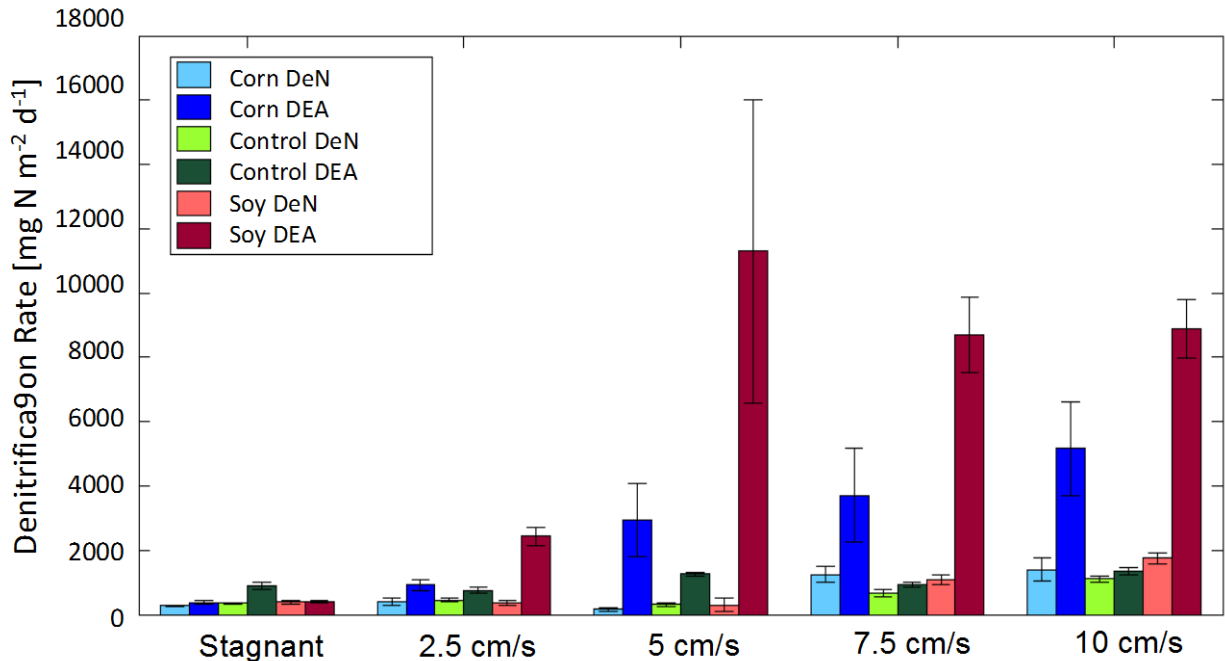


Figure 30. Denitrification potential under flume conditions (DeN) and with nutrients added (DEA) using the acetylene block for the three sediment types and four velocity experiments.

Nitrate concentrations were measured consistently in flume water to determine a nitrate uptake rate from nitrate loss in the flume (Figure 30). This comparison showed that the fastest uptake rates were at the two slower velocities (2.5 and 5 cm/s). Similar results were found previously where nitrate uptake has an optimal rate at a mid-range shear velocity (O'Connor and Hondzo, 2008). Slow velocities stimulate nitrate uptake by creating diffusion of nitrate into the sediments. At higher velocities, several factors can contribute to the decrease in denitrification including less sediment-water contact time, disruption of the biological community, and increased oxygen delivery.

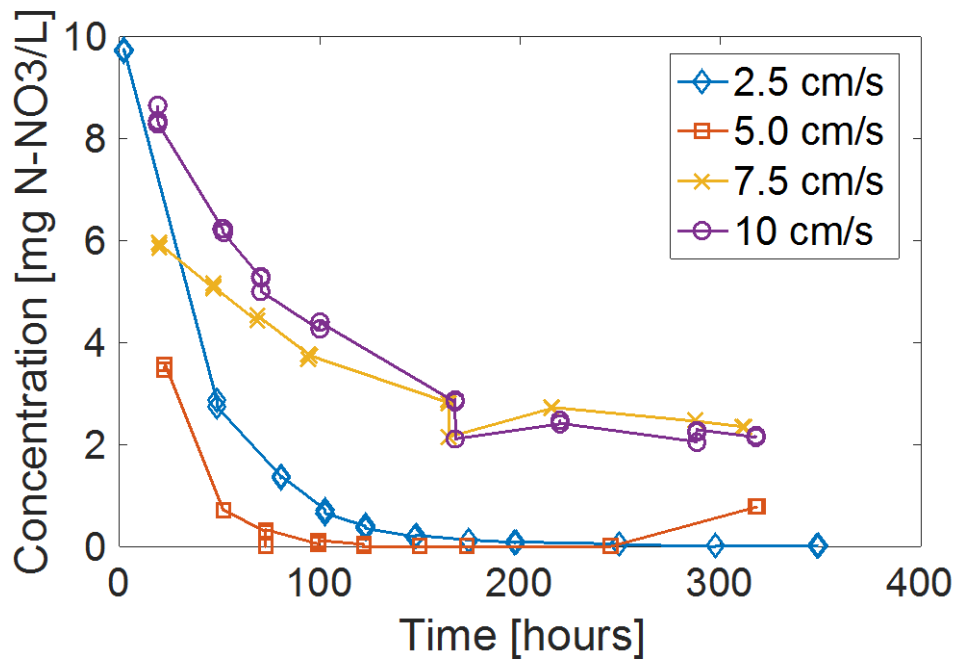


Figure 31. Nitrate concentration over time for the four experimental flume velocities..

In the flume experiments, biofilms began growing on both of the carbon amended soils, whereas no biofilm grew on the control sediment (Figure 32). Also, the biofilms growing on the corn-amended and soy-amended soil appeared different. Samples were taken and viewed under a microscope. The biofilm appears to be composed of diatoms. This biofilm development also altered the velocity profiles over each sediment treatment (Figures 33-35).

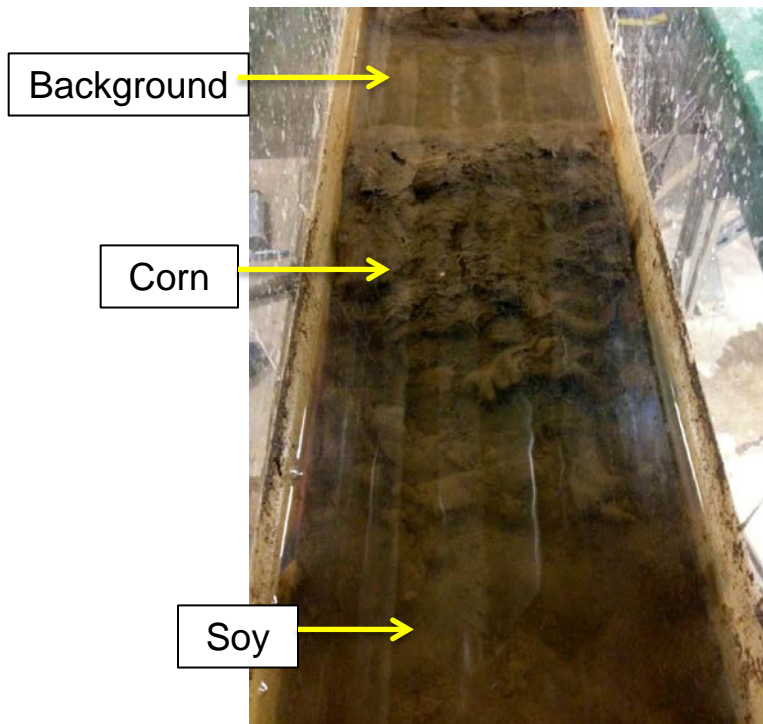


Figure 32. Biofilm growth on flume sediments over the three sediment types.

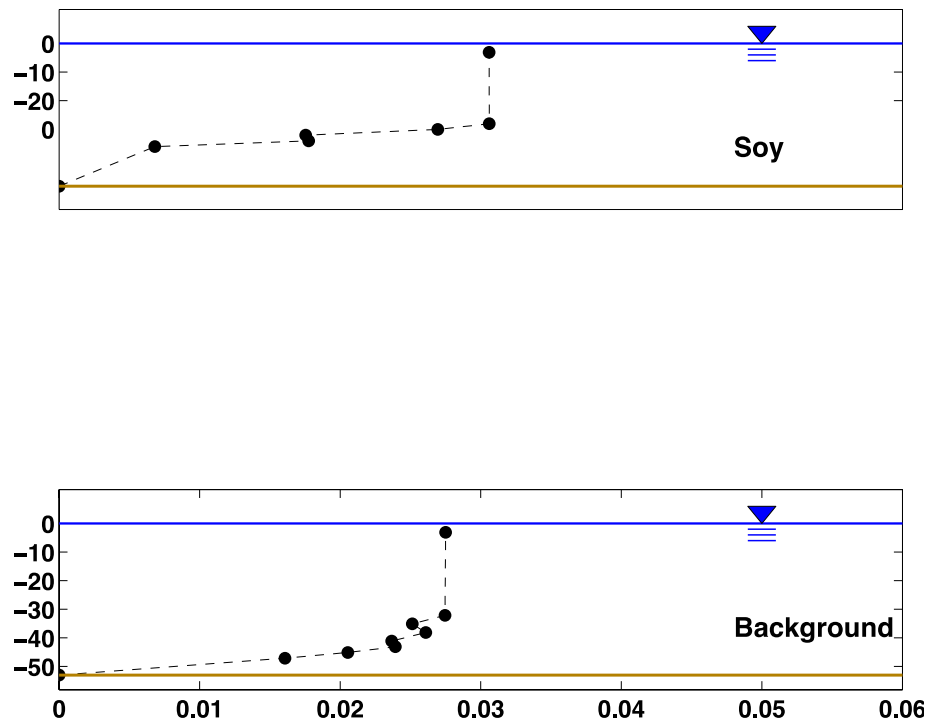


Figure 33. Velocity profiles over each treatment for 2.5 cm/s.

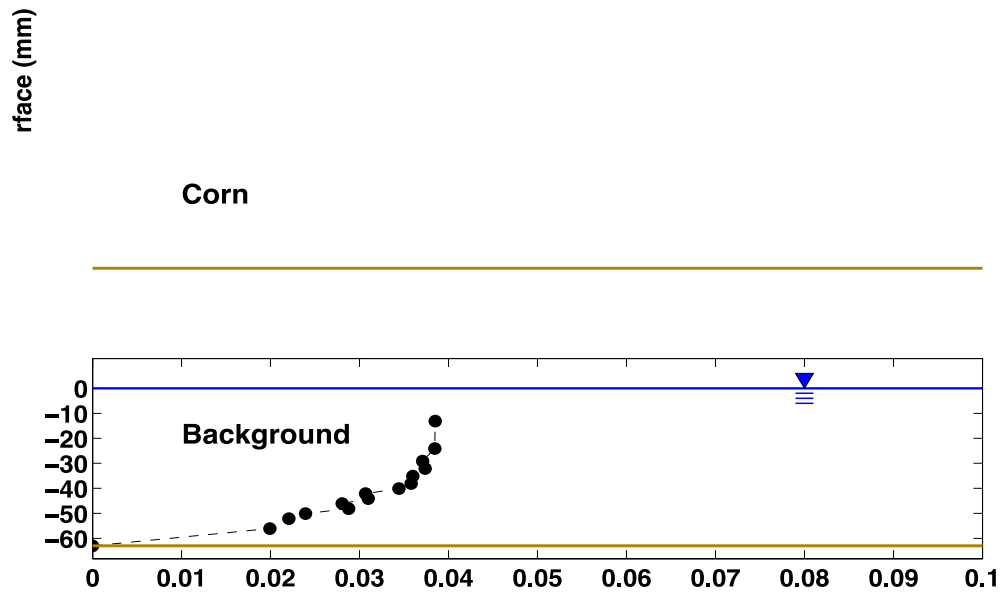


Figure 34. Velocity profiles over each treatment for 5 cm/s.

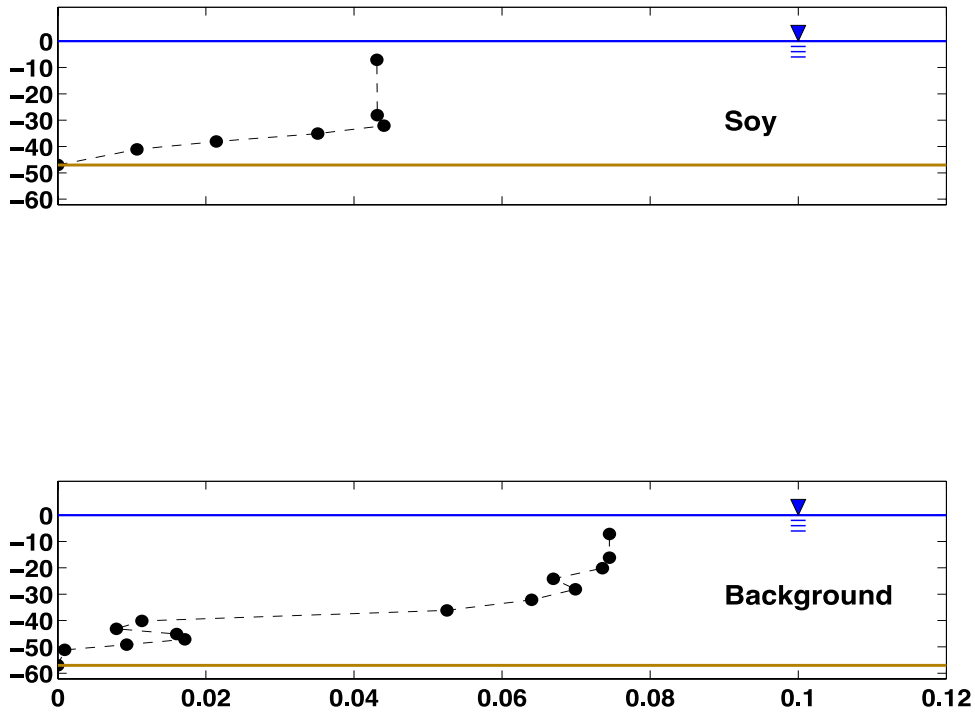


Figure 35. Velocity profiles over each treatment for 7.5 cm/s.

DO profiles collected using a fiber optic DO needle (preSens) showed anoxic conditions in the sediment (Figure 36). The effects of the biofilm growth can also be seen in this figure with the different heights where the conditions turned anoxic. Based on these results, it appears that there were anoxic conditions in the biofilm.

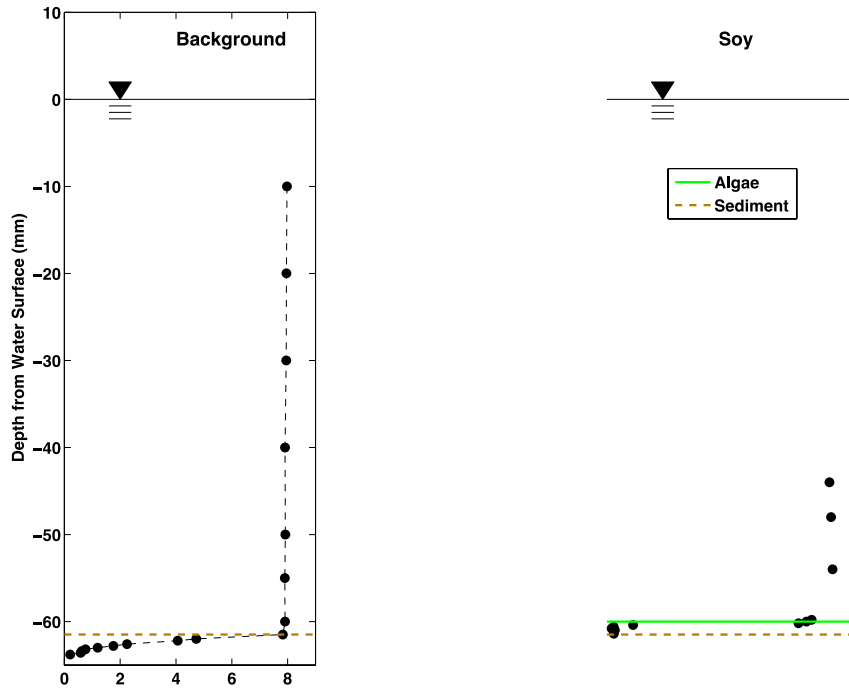


Figure 36. DO profiles in each treatment during 5 cm/s.

## 6 Scaling analysis

Combing results from the flume, OSL, and field studies indicates that denitrification is dependent on several independent environmental parameters (shear velocity, moisture content, organic matter, etc.). A scaling analysis was performed to combine the effects of several parameters by grouping the parameters to form dimensionless groups. These dimensionless groups were then combined to develop functional relationships for denitrification rates. Because the IC, FZ, and NFZ sites displayed different coupling between environmental parameters and denitrification, two equations were created, one for in-channel sites, and another for floodzone and non-floodzone sites. These equations enable denitrification rates to be estimated from easily measureable environmental parameters.

Dimensionless groups were formed using Buckingham's  $\pi$  theorem (Buckingham, 1914, Guentzel et al., 2014, O'Connor et al., 2006). DeN rates were first compared to several controlling environmental parameters (Figure 37 for in-channel and Figure 38 in floodzone and non-floodzone locations). To determine the equations for the in-channel nitrate removal model,

the in-channel dimensionless nitrate uptake  $\left(\frac{DeN}{u_* C_{NO_3}}\right)$  was plotted against the dimensionless Reynolds's number  $\left(\frac{u_* H}{\nu}\right)$ , dimensionless carbon ratio  $\left(\frac{OM}{MC}\right)$ , and dimensionless interstitial space  $\left(\frac{\rho_b}{C_{NO_3}}\right)$  (Figure 39). Similarly, the floodzone and non-floodzone dimensionless nitrate uptake  $\left(\frac{DeN}{ET \rho_b}\right)$  was plotted against dimensionless evapotranspiration  $\left(\frac{ET w}{\nu_{air}}\right)$ , and the dimensionless carbon ratio  $\left(\frac{OM}{MC}\right)$  to determine the equations for the floodzone and non-floodzone nitrate removal model (Figure 40). Exponents for the models were determined by fitting equations for each dimensionless variable versus the dimensionless nitrate uptake. The overall trends using these relationships are depicted in Equations 1 and 2 and are plotted against the dimensionless nitrate uptake in Figure 41 and Figure 42. The dimensionless relationships were plotted on a log-log plot and described 73% of the variation for the in-channel locations and 90% of the variation for the floodzone and non-floodzone locations.

$$\left\langle \frac{DeN}{u_* C_{NO_3}} \right\rangle = 10^{-\frac{7}{4}} \left\langle \frac{u_* H}{\nu} \right\rangle^{-\frac{5}{4}} \left\langle \frac{OM}{MC} \right\rangle^{\frac{7}{2}} \left\langle \frac{\rho_b}{C_{NO_3}} \right\rangle^{\frac{3}{4}} \quad (1)$$

$$\left\langle \frac{DeN}{\rho_b ET} \right\rangle = 10^{-\frac{9}{2}} \left\langle \frac{ET w}{\nu_{air}} \right\rangle^{-\frac{4}{5}} \left\langle \frac{OM}{MC} \right\rangle^{\frac{3}{4}} \quad (2)$$

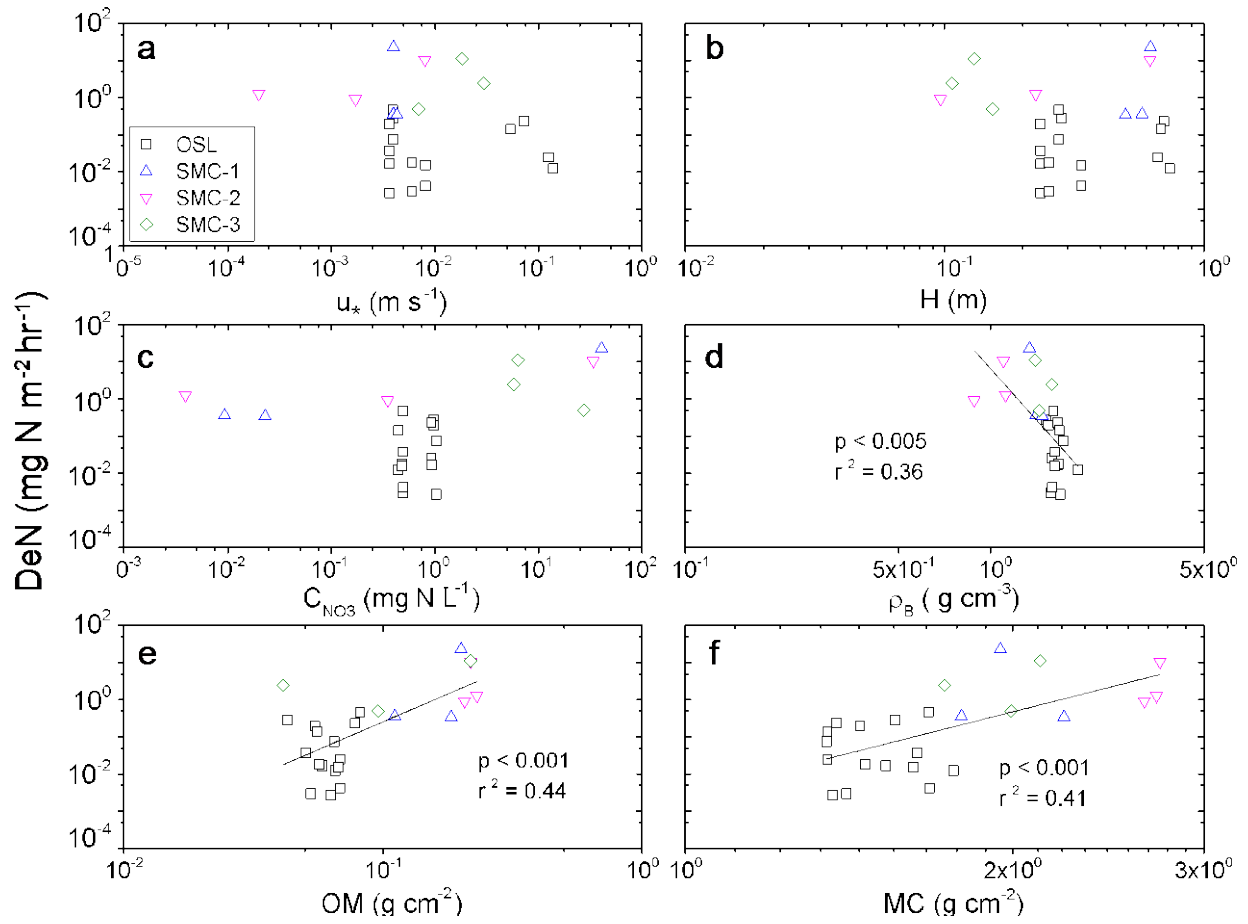


Figure 37. DeN as a function of individual parameters including (a) stream shear velocity ( $u_*$ ), (b) water depth ( $H$ ), (c) water nitrate concentration ( $C_{NO_3}$ ), (d) bulk density ( $\rho_b$ ), (e) organic matter ( $OM$ ), and (f) sediment moisture content ( $MC$ ) for in-channel locations in the SMC wa .

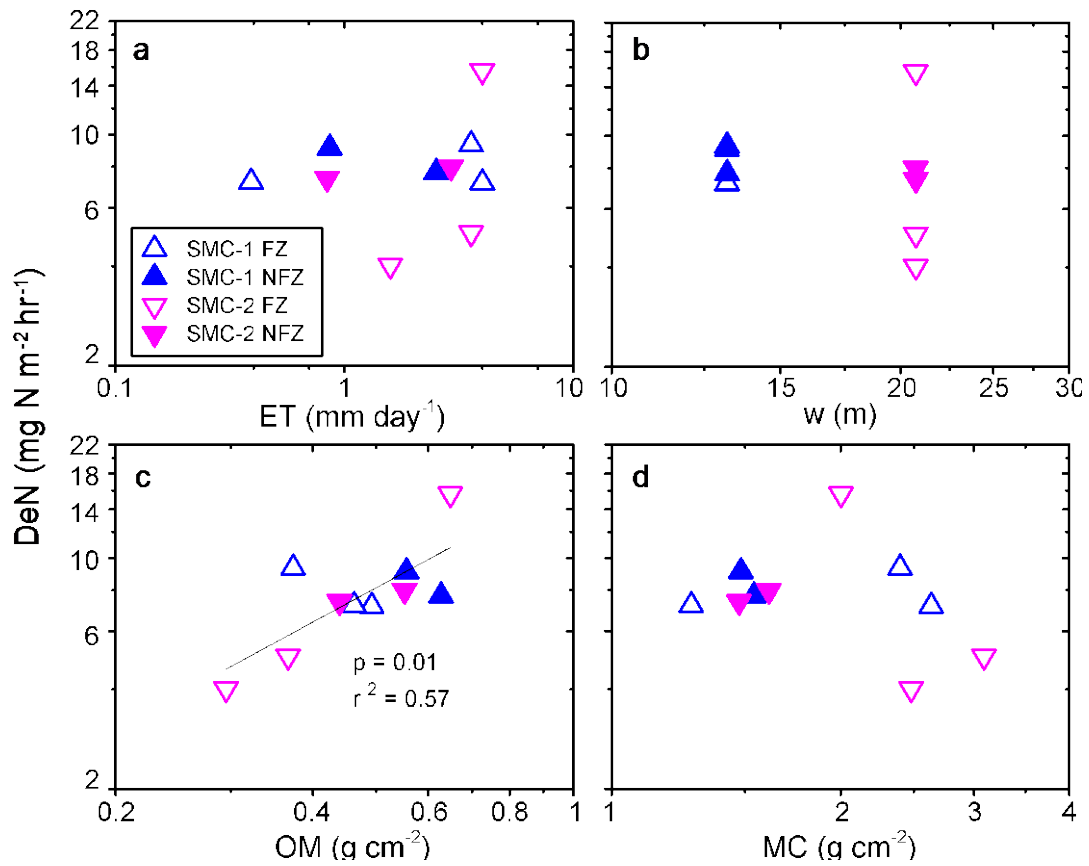


Figure 38. DeN as a function of individual parameters including (a) evapotranspiration (ET), (b) channel top width (w), (c) organic matter (OM), and (d) sediment moisture content (MC) for floodzone (FZ) and non-floodzone (NFZ).

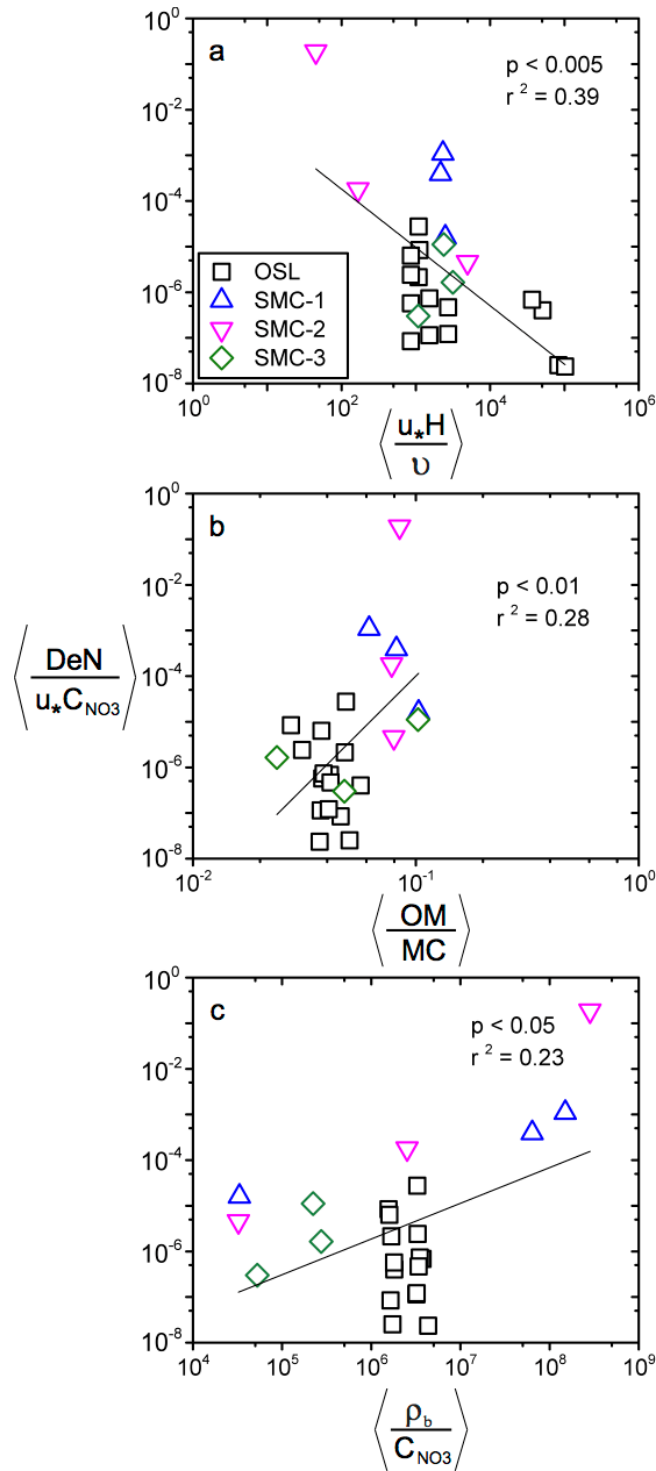


Figure 39. Dimensionless nitrate uptake  $\left\langle \frac{\text{DeN}}{u_* C_{\text{NO}_3}} \right\rangle$  verses (a) dimensionless shear Reynolds number  $\left\langle \frac{u_* H}{\nu} \right\rangle$  (b) dimensionless carbon ratio  $\left\langle \frac{\text{OM}}{\text{MC}} \right\rangle$ , and (c) dimensionless interstitial space  $\left\langle \frac{\rho_b}{C_{\text{NO}_3}} \right\rangle$  for in-channel locations in the Seven Mile Creek (SMC) watershed and the Outdoor StreamLab (OSL).

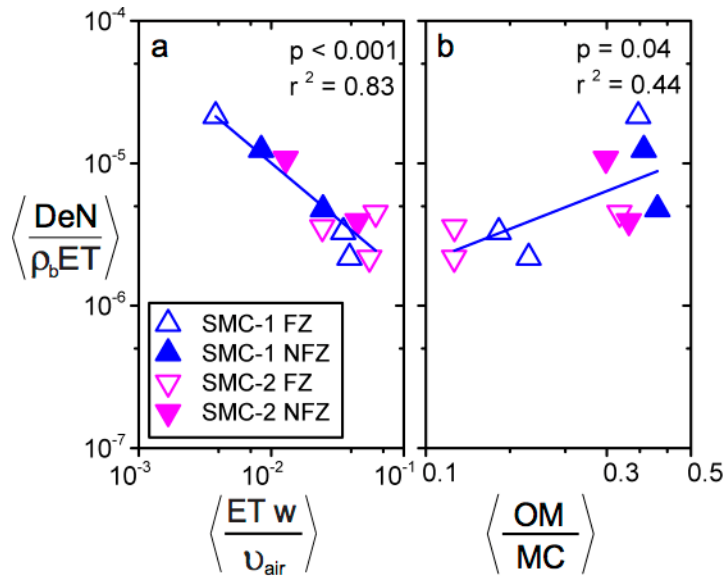


Figure 40. Dimensionless nitrate uptake  $\left\langle \frac{\text{DeN}}{\rho_b \text{ET}} \right\rangle$  verses (a) dimensionless evapotranspiration  $\left\langle \frac{\text{ET } w}{u_{\text{air}}} \right\rangle$ , and (b) dimensionless carbon ratio  $\left\langle \frac{\text{OM}}{\text{MC}} \right\rangle$  for floodzone (FZ) and non-floodzone (NFZ) locations in the Seven Mile Creek (SMC) watershed.

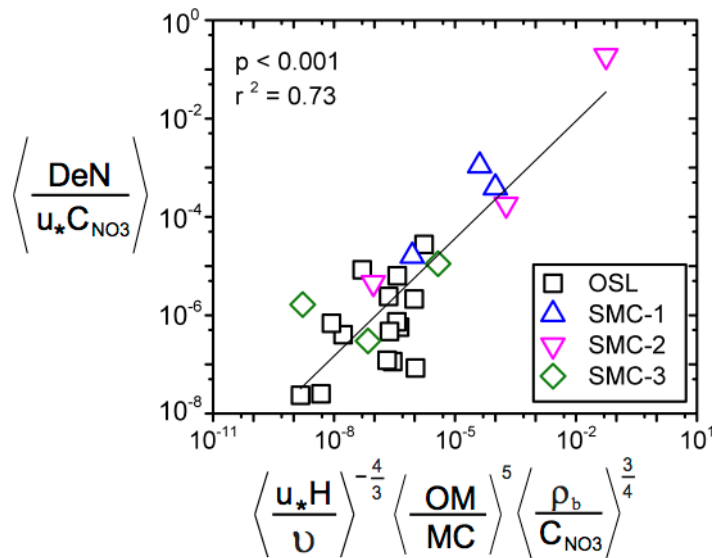


Figure 41. The relationship between dimensionless nitrate uptake, dimensionless shear Reynolds number, dimensionless carbon ratio, and dimensionless interstitial space for in-channel locations in the Seven Mile Creek (SMC) watershed and the Outdoor StreamLab (OSL).

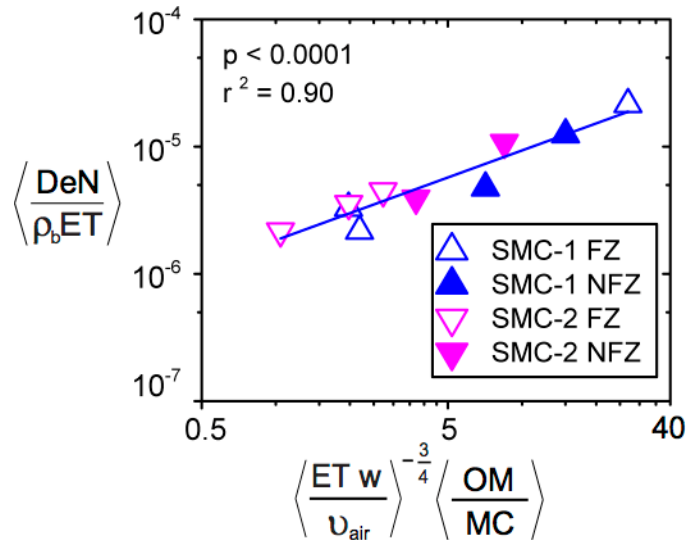


Figure 42. The relationship between dimensionless nitrate uptake, dimensionless evapotranspiration, and dimensionless carbon ratio for floodzone (FZ) and non-floodzone (NFZ) locations in the Seven Mile Creek (SMC) watershed.

## 7 Key Findings

The goal of this project was to identify what drives microbial denitrification hot spots and hot moments in surface water on the Minnesota agricultural landscape, specifically in channels and floodzones (areas that are intermittently flooded with nitrate laden water). Our key findings from combining the results from the flume, field, and OSL experiments are summarized below.

### 7.1 Hot spots and Hot Moments

In-channel, floodzone, and non-floodzone areas generally exhibited different denitrification rates, microbial communities, and abundance of denitrifying genes. Understanding these differences is key to developing BMPs that optimize nitrate removal in agricultural surface waters.

Non-floodzone:

- Relatively stable denitrification rates across sites and seasons.
- Denitrification rates had little response to environmental parameters.
- Low total bacterial abundance and diversity.

In-channel:

- Seasonally variable denitrification rates dependent on nitrate concentration.
- Spatially variable denitrification rates dependent on organic matter concentration.
- Sandy, low organic matter sediment had low total bacterial abundance and diversity.
- Disruptions of mobile sediment lead to decreased denitrification rates.
- Predictive equations combining environmental parameters described the denitrification rates within channel sediments.

Floodzone:

- Periodic inundation leads to greater denitrification potential compared to non-floodzone sites.
- Single flood events lead to hot moments (enhanced denitrification).
- Denitrification rates and bacterial abundance and diversity respond to inundation history.
- Predictive equations combining environmental parameters failed to account for the inundation history and will likely misrepresent the relative denitrification rates.

### **7.1.1 Future Research**

Floodplain areas are often recognized as potential biogeochemical hotspots, but questions remain as to how to optimize denitrification in these areas. Specifically, data from our project were able to illustrate a dynamic response in denitrification in response to flooding. The effect of flooding on denitrification varied based on nitrate concentrations and organic matter content, but for situations with high organic matter and nitrate concentrations, the following responses were observed:

- Denitrification activity was temporally (days) enhanced after a short-term flood (hours) with no corresponding increase in microbial denitrifier abundances (Section 5.2).
- Denitrification activity was enhanced after a long-term flood (week) and remained enhanced (Section 5.3).
- The microbial community responded in the floodplain during a wet year, becoming more similar to the channel community (Sections 5.1.4 and 5.1.5).

To accurately predict floodplain denitrification, more research is required on denitrification response in floodplain areas as a function of flooding history (duration and frequency).

## **7.2 Use of Predictive Equations**

As described above, functional relationships were developed to predict relative denitrification rates in agricultural channels and their floodplains using dimensional analysis. These relationships used environmental parameters including shear velocity, bulk density, aqueous nitrate concentration, water depth, sediment organic matter, and sediment moisture content for the in-channel locations. A similar relationship was developed for non-channel locations using evapotranspiration, bulk density, sediment organic matter, and sediment moisture content. These relationships could be used to model the potential location of denitrification hot spots, to examine how changing environmental conditions would affect denitrification rates, and to compare management options for nitrate removal in surface waters.

### **7.2.1 Limitations**

A potential limitation in the use of the developed predictive equations is their application across space and time scales. The in-channel equation developed for the 2014 field data also fit 2015 field data and was similar to an equation developed previously in our research group (Guentzel et al., 2014). This suggests that in-channel sites behave under relatively stable (steady-state) conditions. In contrast, the developed equation for floodplains (using the floodzone and non-floodzone sites) using 2014 field data did not fit the 2015 field data, suggesting unsteady

conditions. This can also be supported when comparing Tables 6 and Table 7, where in 2014 few significant relationships existed between gene abundances, denitrification rates, and environmental parameters at the floodzone location, whereas in 2015, multiple relationships existed. Field conditions in 2014 and 2015 were very different, with extensive and historic flooding occurring between the June and August sampling date in 2014. Our results from the OSL also suggest that floodzone locations are dynamic and are affected by the history of flooding at a site, which our equations did not take into account. Future research will look further into the effect of flooding history (timing and duration) to strengthen this floodplain equation in order to gain a better predictive tool to estimate nitrate removal in agricultural landscapes.

- The in-channel predictive equation should be limited to low-gradient channels that are always inundated.
- Denitrification rates are relative based on common methods of measurement, and should not be used to represent deterministic values of nitrate removal.
- This equation has not been tested outside of this geographic region and needs to be verified before being applied elsewhere.
- The floodplain equation represents relative denitrification rates based on periodic inundation, but should not be used in abnormally wet years with frequent or long-term inundation.

## **8 Recommendations**

From this research, several factors were found that increased denitrification and could be applied towards remediation strategies. These potential remediation strategies include targeting areas with low-organic sediment and amending the sediment with a carbon source, modifying ditch geometry, and controlling water levels in the ditches. Field and laboratory results all showed that organic sediments had much greater denitrification rates than low organic sediments. A potential remediation strategy to increase nitrate removal would be to target specific areas and amend the sediment with a stable carbon source.

Traditional agricultural ditches are trapezoidal with steep sides. Results from this study showed that denitrification rates at a site that was periodically inundated in a ditch with a depositional floodplain had higher rates of denitrification than at a location that periodically inundated in a trapezoidal ditch. Also, results showed that periodic inundation increased denitrification rates. Therefore, remediation strategies that create sites that periodically flood, and especially strategies that include constructed floodplains, have the potential to increase nitrate removal in agricultural ditches. One potential example of this is constructed two-stage ditches. These practices have the added benefit of slower flows, more reactive surface area, and paired nitrification-denitrification, all leading to enhanced denitrification rates. Also, with slower flows, more sediment will settle, reducing suspended solid and phosphorus loading, and potentially increasing sediment organic matter. Another remediation strategy would be water level control in the ditches. Controlling water level would allow for slower flows through the ditch, reducing shear stress and allowing for more sediment water contact time. This would also allow for controlled pulse flows of ditch water. As seen from the OSL results, short-term pulse flows have the potential of increasing denitrification rates, especially in time periods with high water nitrate conditions.

Even with these remediation strategies, it is important to note that nitrate concentrations in ditch water is often so high that these practices alone are not enough to decrease nitrate levels to an acceptable level through denitrification. For instance, Roley et al. (2012a) showed that even if all of the stream length in a subwatershed in Indiana were placed in a two-stage configuration, nitrate reductions would be only 10% of the annual load. For this reason, a combination of practices should be used to reduce high nitrate loads in the agricultural Midwest. Headwaters need to be targeted since headwaters, with their shallower and slower flows, have a higher potential for denitrification than higher order streams. However, we do not have enough kilometers of headwater to remove nitrate through denitrification, emphasizing that on-field practices are necessary if we are to solve the nitrate problem.

## 9 References

- Alexander, R. B., Bohlke, J. K., Boyer, E. W., David, M. B., Harvey, J. W., Mulholland, P. J., Seitzinger, S. P., Tobias, C. R., Tonitto, C. and Wollheim, W. M. (2009) 'Dynamic modeling of nitrogen losses in river networks unravels the coupled effects of hydrological and biogeochemical processes', *Biogeochemistry*, 93(1-2), pp. 91-116.
- Arango, C. P., Tank, J. L., Schaller, J. L., Royer, T. V., Bernot, M. J. and David, M. B. (2007) 'Benthic organic carbon influences denitrification in streams with high nitrate concentration', *Freshwater Biology*, 52(7), pp. 1210-1222.
- Arnon, S., Gray, K. A. and Packman, A. I. (2007) 'Biophysicochemical process coupling controls nitrate use by benthic biofilms', *Limnology and Oceanography*, 52(4), pp. 1665-1671.
- Barrett, M., Jahangir, M., Lee, C., Smith, C., Bhreathnach, N., Collins, G., Richards, K. and O'Flaherty, V. (2013) 'Abundance of denitrification genes under different peizometer depths in four Irish agricultural groundwater sites', *Environmental Science and Pollution Research*, 20(9), pp. 6646-6657.
- Bernot, M. J., Dodds, W. K., Gardner, W. S., McCarthy, M. J., Sobolev, D. and Tank, J. L. (2003) 'Comparing denitrification estimates for a texas estuary by using acetylene inhibition and membrane inlet mass spectrometry', *Applied and Environmental Microbiology*, 69(10), pp. 5950-5956.
- Biron, P. M., Robson, C., Lapointe, M. F. and Gaskin, S. J. (2004) 'Comparing different methods of bed shear stress estimates in simple and complex flow fields', *Earth Surface Processes and Landforms*, 29(11), pp. 1403-1415.
- Black C.A. 1965. "Methods of Soil Analysis: Part I Physical and mineralogical properties". American Society of Agronomy, Madison, Wisconsin, USA.
- Braker, G. and Conrad, R. (2011) 'Diversity, Structure, and Size of N<sub>2</sub>O-Producing Microbial Communities in Soils-What Matters for Their Functioning?', in Laskin, A.I., Sariaslani, S. & Gadd, G.M. (eds.) *Advances in Applied Microbiology, Vol 75 Advances in Applied Microbiology*. San Diego: Elsevier Academic Press Inc, pp. 33-70.
- Buckingham, E. 1914. On physically similar systems: illustrations of the use of dimensional equations. *Physical Review*.
- Bukaveckas, P. A. (2007) 'Effects of channel restoration on water velocity, transient storage, and nutrient uptake in a channelized stream', *Environmental Science & Technology*, 41(5), pp. 1570-1576.

- Camargo, J. A. and Alonso, A. (2006) 'Ecological and toxicological effects of inorganic nitrogen pollution in aquatic ecosystems: A global assessment', *Environment International*, 32(6), pp. 831-849.
- Caporaso, J. G., Lauber, C. L., Walters, W. A., Berg-Lyons, D., Huntley, J., Fierer, N., Owens, S. M., Betley, J., Fraser, L., Bauer, M., Gormley, N., Gilbert, J. A., Smith, G., Knight, R. (2012) 'Ultra-high-throughput microbial community analysis on the Illumina HiSeq and MiSeq platforms', *ISME J* 6:1621–1624.
- Correa-Galeote, D., Tortosa, G. and Bedmar, E. J. (2013) 'Determination of denitrification genes abundance in environmental samples', *Metagenomics*, 2, pp. 1-14.
- Dingman, S. L. (2008) *Physical Hydrology*. Second ed. Long Grove, IL: Waveland Press, Inc.
- Fageria, N. K. and Baligar, V. C. (2005) 'Enhancing nitrogen use efficiency in crop plants', in Sparks, D.L. (ed.) *Advances in Agronomy, Vol 88 Advances in Agronomy*. San Diego: Elsevier Academic Press Inc, pp. 97-185.
- Gardner, W. H. (1986) Water content. In: (ed. A. Klute) *Methods of Soil Analysis, Part 1. Bibliography 165 Physical and Mineralogical Methods*. Agronomy Monograph No.9 (2<sup>nd</sup> edn). pp493-544.
- Groffman, P. M., Altabet, M. A., Bohlke, J. K., Butterbach-Bahl, K., David, M. B., Firestone, M. K., Giblin, A. E., Kana, T. M., Nielsen, L. P. and Voytek, M. A. (2006) 'Methods for measuring denitrification: Diverse approaches to a difficult problem', *Ecological Applications*, 16(6), pp. 2091-2122.
- Groffman, P. M., Butterbach-Bahl, K., Fulweiler, R. W., Gold, A. J., Morse, J. L., Stander, E. K., Tague, C., Tonitto, C. and Vidon, P. (2009) 'Challenges to incorporating spatially and temporally explicit phenomena (hotspots and hot moments) in denitrification models', *Biogeochemistry*, 93(1-2), pp. 49-77.
- Guentzel, K. S., Hondzo, M., Badgley, B. D., Finlay, J. C., Sadowsky, M. J. and Kozarek, J. L. (2014) 'Measurement and Modeling of Denitrification in Sand-Bed Streams under Various Land Uses', *Journal of Environmental Quality*, 43(3), pp. 1013-1023.
- Guo, X. B., Drury, C. F., Yang, X. M., Reynolds, W. D. and Fan, R. Q. (2014) 'The Extent of Soil Drying and Rewetting Affects Nitrous Oxide Emissions, Denitrification, and Nitrogen Mineralization', *Soil Science Society of America Journal*, 78(1), pp. 194-204.
- Heiri, O., Lotter, A. F. and Lemcke, G. (2001) 'Loss on ignition as a method for estimating organic and carbonate content in sediments: reproducibility and comparability of results', *Journal of Paleolimnology*, 25(1), pp. 101-110.
- Inwood, S. E., Tank, J. L. and Bernot, M. J. (2007) 'Factors controlling sediment denitrification in midwestern streams of varying land use', *Microbial Ecology*, 53(2), pp. 247-258.
- Kazemzadeh, A. and Ensafi, A. A. (2001) 'Sequential flow injection spectrophotometric determination of nitrite and nitrate in various samples', *Analytica Chimica Acta*, 442(2), pp. 319-326.
- Loken, L. C., Small, G. E., Finlay, J. C., Sterner, R. W. and Stanley, E. H. (2016) 'Nitrogen cycling in a freshwater estuary', *Biogeochemistry*, 127(2-3), pp. 199-216.
- Lurndahl, N. (2016) *Temporal and spatial trends in the abundance of functional denitrification genes and observed soil moisture and potential denitrification rates*. MS, University of Minnesota, Minneapolis.
- Mahl, U. H., Tank, J. L., Roley, S. S. and Davis, R. T. (2015) 'Two-Stage Ditch Floodplains Enhance N-Removal Capacity and Reduce Turbidity and Dissolved P in Agricultural Streams', *Journal of the American Water Resources Association*, 51(4), pp. 923-940.

- McClain, M. E., Boyer, E. W., Dent, C. L., Gergel, S. E., Grimm, N. B., Groffman, P. M., Hart, S. C., Harvey, J. W., Johnston, C. A., Mayorga, E., McDowell, W. H. and Pinay, G. (2003) 'Biogeochemical hot spots and hot moments at the interface of terrestrial and aquatic ecosystems', *Ecosystems*, 6(4), pp. 301-312.
- Miller, T. P., Peterson, J. R., Lenhart, C. F. , and Nomura, Y. (2012) *The Agricultural BMP Handbook for Minnesota*. Minnesota Department of Agriculture.
- Mulholland, P. J., Helton, A. M., Poole, G. C., Hall, R. O., Jr., Hamilton, S. K., Peterson, B. J., Tank, J. L., Ashkenas, L. R., Cooper, L. W., Dahm, C. N., Dodds, W. K., Findlay, S. E. G., Gregory, S. V., Grimm, N. B., Johnson, S. L., McDowell, W. H., Meyer, J. L., Valett, H. M., Webster, J. R., Arango, C. P., Beaulieu, J. J., Bernot, M. J., Burgin, A. J., Crenshaw, C. L., Johnson, L. T., Niederlehner, B. R., O'Brien, J. M., Potter, J. D., Sheibley, R. W., Sobota, D. J. and Thomas, S. M. (2008) 'Stream denitrification across biomes and its response to anthropogenic nitrate loading', *Nature*, 452(7184), pp. 202-U46.
- O'Connor, B. and Hondzo, M. (2008) 'Enhancement and inhibition of denitfication by fluid-flow and dissolved oxygen flux to stream sediments', *Environmental Science & Technology*, 42(1), pp. 119-125.
- O'Connor, B. L., Harvey, J. W. and McPhillips, L. E. (2012) 'Thresholds of flow-induced bed disturbances and their effects on stream metabolism in an agricultural river', *Water Resources Research*, 48, pp. 18.
- O'Connor, B. L., Hondzo, M., Dobraca, D., LaPara, T. M., Finlay, J. C. and Brezonik, P. L. (2006) 'Quantity-activity relationship of denitrifying bacteria and environmental scaling in streams of a forested watershed', *Journal of Geophysical Research*, 111.
- Peralta, A. L., Matthews, J. W. and Kent, A. D. (2014) 'Habitat Specialization Along a Wetland Moisture Gradient Differs Between Ammonia-oxidizing and Denitrifying Microorganisms', *Microbial Ecology*, 68(2), pp. 339-350.
- Perryman, S. E., Rees, G. N., Walsh, C. J. and Grace, M. R. (2011) 'Urban Stormwater Runoff Drives Denitrifying Community Composition Through Changes in Sediment Texture and Carbon Content', *Microbial Ecology*, 61(4), pp. 932-940.
- Pinay, G., Black, V. J., Planty-Tabacchi, A. M., Gumiero, B. and Decamps, H. (2000) 'Geomorphic control of denitrification in large river floodplain soils', *Biogeochemistry*, 50(2), pp. 163-182.
- Pinay, G., Gumiero, B., Tabacchi, E., Gimenez, O., Tabacchi-Planty, A. M., Hefting, M. M., Burt, T. P., Black, V. A., Nilsson, C., Iordache, V., Bureau, F., Vought, L., Petts, G. E. and Decamps, H. (2007) 'Patterns of denitrification rates in European alluvial soils under various hydrological regimes', *Freshwater Biology*, 52(2), pp. 252-266.
- Powlson, D. S., Addisott, T. M., Benjamin, N., Cassman, K. G., de Kok, T. M., van Grinsven, H., L'Hirondel, J. L., Avery, A. A. and van Kessel, C. (2008) 'When does nitrate become a risk for humans?', *Journal of Environmental Quality*, 37(2), pp. 291-295.
- Rabalais, N. N., Turner, R. E., Sen Gupta, B. K., Boesch, D. F., Chapman, P. and Murrell, M. C. (2007) 'Hypoxia in the northern Gulf of Mexico: Does the science support the plan to reduce, mitigate, and control hypoxia?', *Estuaries and Coasts*, 30(5), pp. 753-772.
- Roley, S. S., Tank, J. L., Stephen, M. L., Johnson, L. T., Beaulieu, J. J. and Witter, J. D. (2012a) 'Floodplain restoration enhances denitrification and reach-scale nitrogen removal in an agricultural stream', *Ecological Applications*, 22(1), pp. 281-297.

- Roley, S. S., Tank, J. L. and Williams, M. A. (2012b) 'Hydrologic connectivity increases denitrification in the hyporheic zone and restored floodplains of an agricultural stream', *Journal of Geophysical Research*, 117(G3).
- Sadowsky, M., Matteson, S., Hamilton, M. and Chandrasekaran, R. 2010. Growth, survival, and genetic structure of *E. coli* found in ditch sediments and water at the Seven Mile Creek Watershed 2008-2010. Project Report to Minnesota Department of Agriculture.
- Schloss, P. D., Westcott, S. L., Ryabin, T., Hall, J. R., Hartmann, M., Hollister, E. B., Lesniewski, R. A., Oakley, B. B., Parks, D. H., Robinson, C. J., Sahl, J. W., Stres, B., Thallinger, G. G., Van Horn, D. J., Weber, C.F. (2009) 'Introducing mothur: open-source, platform-independent, community-supported software for describing and comparing microbial communities', *Appl Environ Microbiol* 75:7537–7541.
- Seitzinger, S. P., Nielsen, L. P., Caffrey, J. and Christensen, P. B. (1993) 'Denitrification measurements in aquatic sediments- a comparison of 3 methods', *Biogeochemistry*, 23(3), pp. 147-167.
- Staley, C, Gould, T. J., Wang, P., Phillips, J., Cotner, J. B., Sadowsky, M. J. (2015) 'Evaluation of water sampling methodologies for amplicon-based characterization of bacterial community structure', *J Microbiol Methods* 114:43–50.
- Thorntwaite, C. W. (1948) 'An approach toward a rational classification of climate', *Geographical Review*, 38(1), pp. 55-94.
- Tiedje, J. (1982) 'Denitrification', in A.L. Page, R.H.M., D.R. Keeney (ed.) *Methods of soil analysis, part 2. Agronomy Monograph no. 9*. Madison, WI: American Society of Agronomy, pp. 1011-1026.
- Tiedje, J. M., Simkins, S. and Groffman, P. M. (1989) 'Perspectives on measurement of denitrification in the field including recommended protocols for acetylene based methods', *Plant and Soil*, 115(2), pp. 261-284.
- Turner, R. E., Rabalais, N. N. and Justic, D. (2006) 'Predicting summer hypoxia in the northern Gulf of Mexico: Riverine N, P, and Si loading', *Marine Pollution Bulletin*, 52(2), pp. 139-148.
- Ward, M. H., Kilfoy, B. A., Weyer, P. J., Anderson, K. E., Folsom, A. R. and Cerhan, J. R. (2010) 'Nitrate Intake and the Risk of Thyroid Cancer and Thyroid Disease', *Epidemiology*, 21(3), pp. 389-395.
- Yu, K. W., Seo, D. C. and DeLaune, R. D. (2010) 'Incomplete Acetylene Inhibition of Nitrous Oxide Reduction in Potential Denitrification Assay as Revealed by using <sup>15</sup>N-Nitrate Tracer', *Communications in Soil Science and Plant Analysis*, 41(18), pp. 2201-2210.
- Zhu, G. B., Wang, S. Y., Wang, W. D., Wang, Y., Zhou, L. L., Jiang, B., Op den Camp, H. J. M., Risgaard-Petersen, N., Schwark, L., Peng, Y. Z., Hefting, M. M., Jetten, M. S. M. and Yin, C. Q. (2013) 'Hotspots of anaerobic ammonium oxidation at land-freshwater interfaces', *Nature Geoscience*, 6(2), pp. 103-107.
- Zumft, W. G. (1997) 'Cell biology and molecular basis of denitrification', *Microbiology and Molecular Biology Reviews*, 61, pp. 533-616.